An Evaluation of a Methodology for the Detection of Leaks in Aboveground Storage Tanks

HEALTH AND ENVIRONMENTAL AFFAIRS
API PUBLICATION NUMBER 325
MAY 1994

STEP
Strategies for Today's Environmental Partnership

American Petroleum Institute
1220 L Street, Northwest
Washington, D.C. 20005

An Evaluation of a Methodology for the Detection of Leaks in Aboveground Storage Tanks

Health and Environmental Affairs Department

API PUBLICATION NUMBER 325

PREPARED UNDER CONTRACT BY:
MICHAEL R. FIERRO
ERIC G. ECKERT
JOSEPH W. MARESCA, JR.

VISTA RESEARCH, INC.
MOUNTAIN VIEW, CALIFORNIA

MAY 1994

American
Petroleum
Institute

FOREWORD

API PUBLICATIONS NECESSARILY ADDRESS PROBLEMS OF A GENERAL NATURE. WITH RESPECT TO PARTICULAR CIRCUMSTANCES, LOCAL, STATE, AND FEDERAL LAWS AND REGULATIONS SHOULD BE REVIEWED.

API IS NOT UNDERTAKING TO MEET THE DUTIES OF EMPLOYERS, MANUFACTURERS, OR SUPPLIERS TO WARN AND PROPERLY TRAIN AND EQUIP THEIR EMPLOYEES, AND OTHERS EXPOSED, CONCERNING HEALTH AND SAFETY RISKS AND PRECAUTIONS, NOR UNDERTAKING THEIR OBLIGATIONS UNDER LOCAL, STATE, OR FEDERAL LAWS.

NOTHING CONTAINED IN ANY API PUBLICATION IS TO BE CONSTRUED AS GRANTING ANY RIGHT, BY IMPLICATION OR OTHERWISE, FOR THE MANUFACTURE, SALE, OR USE OF ANY METHOD, APPARATUS, OR PRODUCT COVERED BY LETTERS PATENT. NEITHER SHOULD ANYTHING CONTAINED IN THE PUBLICATION BE CONSTRUED AS INSURING ANYONE AGAINST LIABILITY FOR INFRINGEMENT OF LETTERS PATENT.

ACKNOWLEDGMENTS

We wish to thank the members of the API Storage Tank Task Force, Work Group for AST Monitoring, for their cooperation, their technical support, and their assistance in coordinating the project. We would like to acknowledge the support and encouragement of Mr. James Seebold, the chairperson of the Work Group, and of Ms. Dee Gavora and Andrew Jaques of the Health and Environmental Affairs Department, the API staff members monitoring the program.

We would also like to acknowledge the contributions of the following individuals, companies/individuals: Steve Tostengard, Jerry Engelhardt and Vince Rosero of Santa Fe Pacific Pipeline Partners, Inc., for the use of their company's terminal, and their invaluable assistance in coordinating the field test effort; Robert Brozovich, Gordon Ray and Chuck Hill, also of SFPP, for their efforts in planning and scheduling the experimental work; Bill Matney, Jim Eschberger and Glenn Kauffman for their operational support; Jim Leaird and Dennis Biddle of Physical Acoustics Corporation; and David Waterman and Ralph Nicastro of Rohrback Cosasco System, Inc.

We would also like to acknowledge Gregg Olson and Richard Wise of Vista Research for their assistance in conducting the field test activities, and Monique Seibel and Christine Lawson of Vista Research for their efforts in editing and typesetting this document.

TABLE OF CONTENTS

LIST OF FIGURES

Figure

LIST OF TABLES

Table

EXECUTIVE SUMMARY

INTRODUCTION

The American Petroleum Institute has undertaken a significant technical effort to define and advance the state of the art of leak detection in aboveground storage tanks (ASTs). This report presents the results of Phase IV of the API leak detection program. The three research efforts that preceded Phase IV were focused on the assessment of leak detection technology for ASTs and a detailed evaluation of passive acoustic and volumetric measurement methods. Field tests conducted on operational ASTs as part of the Phase III effort demonstrated that accurate leak detection could be accomplished through acoustic and volumetric techniques, and suggested specific changes in system design and test protocol to improve the performance of each technology. Based upon the Phase III results, general recommendations were made regarding further experimental work.

In addition, a methodology was developed which combines multiple AST testing technologies in order to assess the integrity of an AST. The proposed methodology may also include multiple tests with each technology. This methodology is designed to verify the presence of a leak in the case of a detection, and thereby minimize the occurrence of erroneous decisions based on test results which indicate the presence of a leak when none exist (false alarms). Effectively combining independent test methods should result in a very robust leak detection practice. Three leak detection techniques were selected for evaluation in the Phase IV program: passive-acoustics, volumetric methods (including both level-and-temperature and mass measurement systems), and soil-vapor monitoring. Though soil-vapor monitoring was not evaluated in the previous phases of API's research, it was identified as a technology of interest to the industry and was included in this phase. Individually, all three of these technologies are believed to have the potential for reliably detecting small leaks in the floor of an AST. When used together, the reliability of the test results increases.

Other AST leak detection technologies exist, and new technologies and new implementation techniques are being developed. Other technologies may perform equally well in a similar test methodology; however, API has limited the focus of this research to the three technologies mentioned above. The test methodology presented here is one example of a method to improve the reliability of a test decision through the used of multiple testing techniques.

The proposed leak detection methodology was applied to 14 ASTs during an eight-week period between 15 March and 3 May, 1993, at a facility provided by Santa Fe Pacific Pipeline Partners, Inc..

The objectives of the Phase IV study were:

- to assess the applicability of the general features of the three AST leak detection technologies (acoustic, volumetric, and soil-vapor monitoring technologies) over a wide range of tank types, petroleum fuels, and operational conditions
- to assess the applicability of a general leak testing methodology for ASTs which involves multiple tests at multiple product levels in the tanks
- to determine the integrity of 14 ASTs using two or more test methods

CONCLUSIONS

Based on the results of all tests performed, none of the 14 ASTs tested is believed to be leaking. Since there were no indications of a leak, the performance of the proposed test methodology could not be directly evaluated for its effectiveness in reducing false alarms or missed detections. Based on a study of the noise environment for each of the test methods included in the methodology, however, the proposed methodology is believed to have met the requirements for incorporating independent test methods with reasonable probabilities of detection.

The results of passive-acoustic testing performed in this test series indicates that the data collection and analysis approach based on the recommendations from Phase III, and demonstrated in this program, can be employed on a wide range of tanks with a low probability of false alarm. Acoustic leak detection tests differentiate acoustic leak signals from impulsive noise events primarily on the basis of the estimated spatial origin of the signal and on its duration. A detection is made when a number of acoustic events are located in an area on the tank floor that is consistent with the location accuracy of the acoustic sensor array. The two sources of false hits, which can lead to false detections, are non-leak sources of impulsive acoustic signals generated at the floor of an AST, and the mislocation of impulsive acoustic signals that originate from locations other than the floor of the tank (e.g., the product surface, tank shell, tank roof, etc.). The data collection and analysis approach used in this test series yielded no false events in any of the 14 ASTs tested. This is an extremely important result, because until now implementations of acoustic technology have required that a test decision be made even though there may be many hundreds of false events indicated in the data. The primary noise sources identified in this test series originated at the product surface, and were due to condensate dripping on the product surface and noise associated with the motion of the ASTs' floating roofs. No impulsive noise sources were found to have originated from the tank floor, even though all of the tanks tested had some internal floor-mounted structure. This is also an important result, because noise sources at the floor of an AST could be difficult to distinguish from a leak signal. In the 14 ASTs tested, it was found that all noise sources recorded could be spatially discriminated from any possible leak signal through analysis of digital time series of the acoustic waveform.

The soil-vapor monitoring test applied in Phase IV used pentane, which was present in the petroleum fuel, as the target vapor. Two types of hydrocarbon sampling systems tuned for the detection of pentane were used: a fiber optic sensor system capable of measuring concentrations of pentane on the order of 5 ppm, and a gas chromatograph capable of measurements to 1 ppm. The results of the pentane injection test performed as part of the series of soil-vapor monitoring tests indicated that pentane propagation through the oiled-sand backfill under the tanks at the test site was too low for a leak to be reliably detected. In order to gain a better understanding of the propagation characteristics of pentane, additional injection tests were performed at another site where the backfill material was sand that had not been oiled and was therefore much more permeable. This second series of injection tests resulted in a much more reliable detection of the injected pentane. While soil-vapor monitoring techniques can potentially be used to detect leaks in ASTs, it is apparent that the soil conditions at the test site limited the effectiveness of this technique. The effect of soil conditions on test variability could be mitigated through the use of longer test periods and a more stable substance as the target vapor. In order for this technology to be effective operationally, and to achieve a reasonable probability of detection, the spacing of sensor wells and the duration of the monitoring period must be carefully chosen. For best results, these decisions should be based on the propagation characteristics of the target vapor as measured at the test site prior to the conduct of a leak detection test. The other important source of error is the presence of water at the bottom of the AST during a test. Unless water is removed, it will prevent the release of pentane and render the test ineffective. Water was drained from all ASTs prior to the start of the Phase IV test series. While the results of the soil-vapor monitoring tests are believed to be valid, there is insufficient information to assess the effects of any residual amount of water left at the bottom of these ASTs.

The performance of volumetric tests, both those that use level-and-temperature measurements and those that use mass-measurement techniques, was consistent with that achieved during the Phase III experiments. While specific noise mechanisms differ in the two types of volumetric tests, the noise in both cases is driven by ambient temperature changes; in the Phase IV test series, the two types of volumetric test had approximately equivalent levels of performance. As in Phase III, it was found that in order to achieve good performance in both types of tests, accurate temperature compensation and test durations greater than 24 h were required.

Section 1

BACKGROUND

The American Petroleum Institute has undertaken a significant technical effort to define and advance the state of the art of leak detection in aboveground storage tanks (ASTs). This report presents the results of Phase IV of the API leak detection program. The three research efforts that preceded Phase IV were focused on the assessment of leak detection technology for ASTs and a detailed evaluation of two leak detection methods: passive acoustics and volumetric measurement (Vista Research, Inc., 1991; Vista Research, Inc., 1992; Vista Research, Inc., 1993a; Vista Research, Inc., 1993b). Field tests conducted on operational ASTs as part of the Phase III effort demonstrated that accurate leak detection could be accomplished through acoustic and volumetric techniques, and suggested specific changes in system design and test protocol to improve the performance of each technology. Based upon the Phase III results, three general recommendations were made regarding further experimental work. First, perform tests on a wide range of operational ASTs using leak detection systems that incorporate the modifications in data collection and analysis suggested by the Phase III results. Second, develop and test a standard procedure for evaluating the performance of volumetric and acoustic leak detection methods in terms of the probability of detection (P_D) and probability of false alarm (P_{FA}). Finally, areas in which volumetric and acoustic methods could benefit from further technological development were identified. The Phase IV effort is intended to address the first of these recommendations. The series of leak detection tests that comprise the Phase IV study were conducted on 14 operational ASTs provided by an API member company in support of the ongoing effort to advance AST leak detection technology. Field test activities for this program were conducted between 13 March and 3 May, 1993. The objectives of this study are:

- to assess the applicability of the general features of the three AST leak detection technologies (acoustic, volumetric, and soil-vapor monitoring) over a broad range of tank types, petroleum fuels, and operational conditions

- to assess the applicability of a general leak testing methodology for ASTs which involves multiple leak detection tests at multiple product levels
- to determine the integrity of 14 ASTs using two or more test methods

The organization of this report is as follows. Section 2 presents a brief description of the leak testing methodology used during the test series. Section 3 contains the specifications (i.e., tank construction and dimensions, product type, etc.) of each of the ASTs tested. Results of the leak detection tests and a summary of the important findings for each of the test methods are presented in Section 4. The conclusions and recommendations derived from these tests are described in Section 5. The final section of this work includes a summary of the general features of system design and test protocol considered to be important with respect to each of the three leak detection technologies investigated. This section is based upon conclusions drawn from all four phases of the API program. Appendices A and B describe, respectively, the technical findings of the acoustic and volumetric experiments performed in Phase IV.

Section 2

TEST METHODOLOGY/ PROPOSED AST LEAK DETECTION PRACTICE

Each of the three leak detection technologies has the potential for reliably detecting small leaks in the floor of an AST. The three techniques are based upon measurements of different aspects of the leak signal, and the noise encountered in each type of test is also very different. The ability of the detection system to recognize the leak signal against the noise ultimately determines the system performance. Effectively combining any two, or all three, of these independent methods should result in a very robust leak detection practice.

Other technologies or implementations of the three technologies other than those investigated in this program may exist or may be developed which will perform equally well alone or when combined into a similar test methodology. It should be stressed that the implementation of the test methodology presented here is intended only as an example of how to improve the reliability of a test decision through the use of multiple independent testing techniques.

The proposed leak testing methodology is based not only on the use of multiple methods but also of multiple tests with each method and multiple levels of product with certain tests. The multiple test strategy, if properly conducted, can significantly increase the reliability of the overall test decision, i.e., whether the tank is leaking or not. The three-step methodology described below is based upon the present understanding of the performance and operational limitations of each of the three technologies.

Step 1. The first step in the proposed leak detection methodology is to test the AST using a relatively non-intrusive technique. In this program, two technologies were used: passive-acoustics and soil-vapor monitoring. The use of these two methods as an initial assessment of tank integrity is desirable since (a) each method should be capable of detecting small leaks under a variety of test conditions, and (b) the impact of the tests on tank operations is minimal. If, as a result of the initial tests, a leak is suspected, another test should be conducted using the same method. This procedure reduces the possibility of a false alarm before a decision is made to proceed to Step 2.

Step 2. The second step in the proposed leak detection methodology, which is taken only after at least two tests in Step 1 indicate the possibility of a leak, is to conduct a volumetric leak detection test with the product level lowered to within 3 to 5 ft of the AST floor. The low product level and the presence of strong diurnal sources of noise require that (a) valves connected to the AST be blinded prior to the test, and (b) the test be at least 24 and preferably 48 h in duration. A tank should not be declared leaking unless two or more volumetric tests give similar indications of a leak.

Step 3. The final step in the proposed leak detection methodology is to remove the tank from service and perform an internal tank inspection. A tank inspection is the current petroleum industry standard for verifying the integrity of the AST floor.

The proposed standardized testing practice for ASTs has, in addition to the improvements in performance described above, a very sound foundation. It terminates in an inspection of the tank bottom, which is the currently accepted practice for making a final decision about the integrity of a tank. This has a subtle but important implication. Regardless of whether there is a real leak or simply a false alarm, the final step in the protocol is the same: tank inspection. Thus, if a lower threshold is selected for the purpose of increasing the probability of detection, the accompanying rise in the rate of false alarm is tolerable, because the alternative would be Step 3 anyway. (At some point, of course, a high false alarm problem will undermine all efforts to test tanks for leaks.) A higher probability of detection favors the environment. Enough is known about the important ("key") features of the three methods that credible threshold selections can be made even if the exact performance of particular systems that operate on the principles of these methods is not known. The proper balance between the P_D and the P_{FA} can be made once the performance of the methods/systems has been evaluated over the range of ambient conditions anticipated during testing.

Section 3

SITE DESCRIPTION

The group of 14 ASTs tested during the API Phase IV effort were of various sizes and construction, and contained diesel, gasoline, turbine, or jet fuel. Any water in the bottom of the ASTs to be tested was drained during the two weeks prior to the start of this test series. All of the tanks were built on an oiled-sand backfill. The tank terminal was bounded by a freeway and a railroad switching yard. A full description of each tested AST is given in Table 3-1.

Table 3-1. AST Summary

AST No.	Product	Nominal Capacity (bbl)	Dia. x Ht. (ft)	Roof Type
2	ULREG	30,000	73 x 40	Float Roof Double Deck
3	MIDGD	20,000	60 x 40	Float Roof Double Deck
7	DIESEL	27,500	70 x 40	Cone Roof
9	TURBINE	20,000	60 x 40	Cone Roof
14	MIDGD	30,000	67 x 48	Float Roof Double Deck
15	ULREG	30,000	67 x 48	Float Roof Double Deck
16	DIESEL	20,000	60 x 40	Float Roof Pontoon Type
18	MIDGD	20,000	60 x 40	Float Roof Double Deck
19	ULREG	20,000	60 x 40	Float Roof Double Deck
22	DIESEL	20,000	54.5 x 48	Float Roof Pontoon Type
23	ULREG	20,000	54.5 x 48	Float Roof Pontoon Type
24	PRM92	10,000	42.5 x 40	Float Roof Pontoon Type
36	JP-4	28,792	67 x 48	Cone Roof Floating Pan
37	JP-5	28,973	67 x 48	Cone Roof Floating Pan

Section 4

RESULTS

The Phase IV program consisted of a set of tests in which the proposed AST leak detection practice was applied to 13 ASTs whose status was not known (the "leak detection tests") and another set of tests in which the three leak detection techniques were used on a 14th AST whose status was known (the "control tests"). The leak detection tests included options for additional data collection when warranted by previous test results. The three leak detection techniques used in the test program were: (1) passive-acoustic tests following the protocol developed as part of the API Phase III field experiments (Vista Research, Inc., 1993a), (2) soil-vapor monitoring tests using pentane (a substance that occurs naturally in the petroleum product) as the target vapor, and (3) volumetric tests (including both level-and-temperature and mass measurements) following the protocol developed as part of the API Phase III field experiments (Vista Research, Inc., 1993b).

Other leak detection techniques -- ones that deviate from the recommendations of the previous API findings -- were also used during Phase IV, and the results of these tests are also included in Section 4. For example, a commercial AST acoustic emissions vendor conducted acoustic tests using that company's standard test protocol, which does not include the collection of waveform time histories as recommended by previous API work. Other AST testing companies conducted high-product-level mass measurement tests and a short-duration mass-measurement test (approximately 4 h). These tests deviate from previous API recommendations that volumetric tests should be conducted at low product levels and that the test should be at least 24 h long.

Tank 23 was chosen as the control tank because it had recently been inspected and was scheduled to be returned to service at the start of this test program. All three leak detection technologies were used to test this tank. The remaining 13 ASTs were tested by means of both acoustic and soil-vapor monitor techniques as the first step of the test methodology. None of the results of these two high-product-level tests indicated the presence of a leak, and therefore, according to the test methodology, no further tests of these tanks were required. Given this result, Tank 9 was chosen arbitrarily for the conduct of the second step in the test methodology, a low-product-level volumetric test. Tank 2 was also selected for volumetric testing. Site personnel, however, required that the floating roof on this tank remain on the product surface. Since this condition violates the test protocol for a volumetric leak detection test, a valid test could not be conducted. Data on Tank 2 were collected nevertheless, and these data were analyzed to assess the impact of a floating roof on volumetric test performance. A complete list of the tests performed on each tank is given in Table 4-1.

Table 4-1. Summary of Tank Tests

Tank No.	Acoustic Test as per Phase III Recommendation	Acoustic Test	Soil-Vapor Monitoring	High-Product-Level Mass Measurement	Low-Product-Level Mass Measurement	Short Duration Low-Product-Level Mass Measurement	Low-Product-Level Level-and-Temperature Measurement
2	✓	✓	✓	✓			✓
3	✓	✓	✓				
7	✓	✓	✓				
9	✓	✓	✓		✓	✓	✓
14	✓	✓	✓				
15	✓	✓	✓				
16	✓	✓	✓				
18	✓	✓	✓				
19	✓	✓	✓				
22	✓	✓	✓				
23[1]	✓	✓	✓	✓	✓		✓
24	✓	✓	✓				
36	✓	✓	✓				
37	✓	✓	✓				

1. Control Test

CONTROL TESTS

The series of control tests was conducted between 14 and 28 March, 1993. The tank had been emptied, cleaned, and inspected prior to the start of testing. The floating roof was resting on its legs at approximately eight feet above the tank floor. On 14 March, three feet of JP-4 fuel was transferred into the tank, and on the following day blinds were installed on all valves connecting pipelines to this tank. Also at this time, four ten-foot sections of pipe (three for soil-vapor monitoring and one for pentane injection) were installed under the AST in a radial pattern at 90° intervals. A 24-h settling period was observed prior to the start of volumetric testing. Volumetric data were collected over a 72-h period from 16 to 19 March. Level-and-temperature and mass-measurement data were collected concurrently during this period. Measured level-and-temperature data showed an average 1.1 gal/h outflow over the three-day period (Figure 4-1). Mass measurement data indicated an outflow of 0.8 gal/h (Figure 4-2). In both tests the most likely cause of the measured outflow is incomplete compensation for the thermal influence from steadily decreasing ambient temperature over the three-day period. Another possibility is loss of product through evaporation; however, the character and rate of the decrease in measured volume do not appear to be consistent with evaporative loss (Vista Research, Inc., 1991).

At the completion of volumetric tests, the valve blinds were removed and the product level in the tank was increased to 35 ft. The blinds were then re-installed in preparation for the high-product-level volumetric test.

Acoustic leak detection tests were conducted on the control tank between 22 and 24 March. Each acoustic test was conducted over a six-hour period that included two hours for setup and system calibration and four hours of data collection. Over the course of this test, all impulsive signals recorded were found to have originated at the product surface and to have been caused by either the motion of the floating roof relative to the AST shell or by condensate dripping down an access port located near the center of the floating roof. No impulsive signals were emitted from the AST floor, indicating that the tank was not leaking.

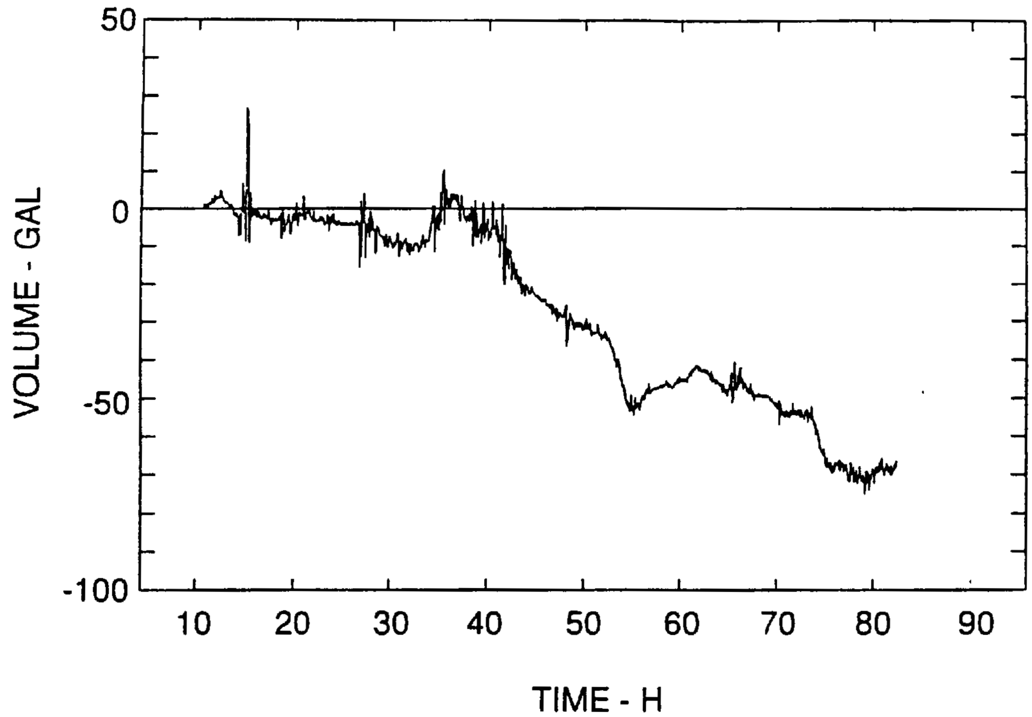

Figure 4-1. Level-and-temperature volumetric data (control tank).

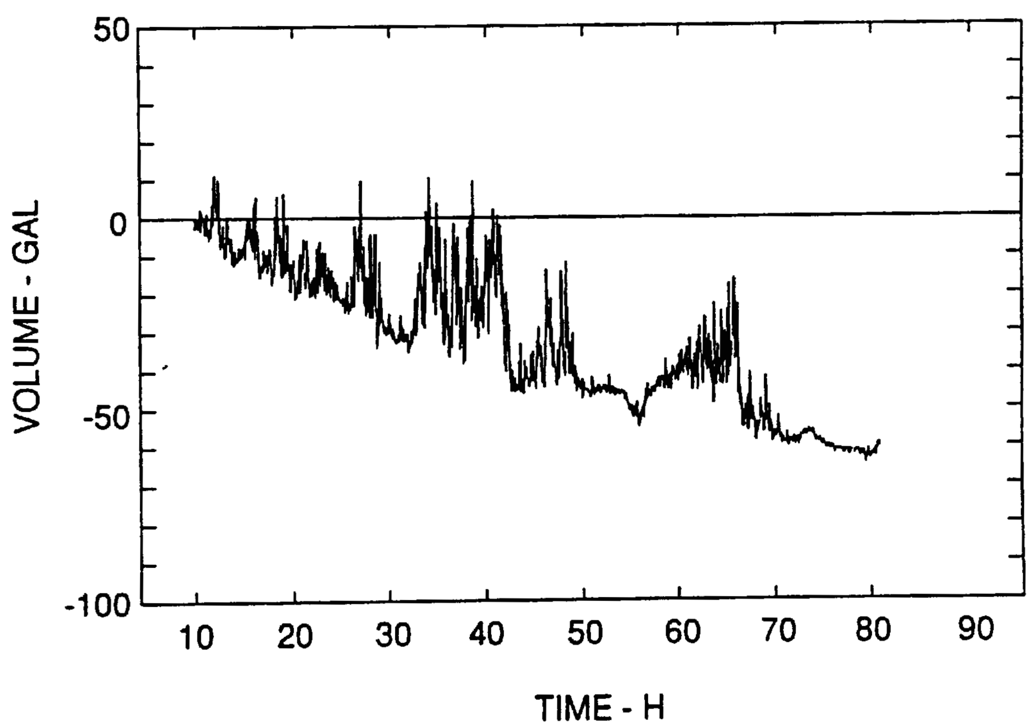

Figure 4-2. Mass-measurement volumetric data (control tank).

Figures 4-3a and 4-3b show, respectively, the location estimates of impulsive events separated into two categories: (1) events which originated from *above* the AST floor and (2) events which originated *on* the AST floor.

In order to verify that the acoustic system was capable of detecting a leak in the AST floor, a leak simulator was installed in the control tank. The leak simulator, when activated, emits impulsive acoustic signals by allowing product to flow through a small orifice into soil contained in the simulator. The air entrapped in the soil creates bubbles that burst in the product flow stream. The signal produced in this way is consistent with observations of real and simulated leak signals made during Phases II and III of the API work (Vista Research, Inc., 1992; Vista Research, Inc., 1993a). Leak detection tests performed on the control tank while the leak simulator was active resulted in the accurate location of the simulator on the AST floor. Figure 4-4a shows the location estimates for recorded impulsive events that originated from above the AST floor and Figure 4-4b for those that originated on the AST floor.

Soil-vapor monitoring tests were conducted during the same period as the acoustic tests. Two types of hydrocarbon sampling systems tuned for the detection of pentane were used: a fiber optic sensor system capable of measuring concentrations of pentane on the order of 5 ppm, and a gas chromatograph capable of measurements to 1 ppm. No detectable levels of pentane were measured with either system at any of the three monitoring wells (sections of pipe) that had been installed beneath the AST. Two gallons of pentane were then injected into the fourth pipe, and suction was applied to the monitoring well located at a 180° angle from the injection well. Suction was applied only during the first eight hours after injection. Twenty hours after the pentane had been injected, levels of 3 to 4 ppm of pentane were measured at the 180° monitoring well, and levels of 1 to 3 ppm were recorded at the other two monitoring wells. Ten days after the pentane had been injected, pentane levels at all wells were below 2 ppm. All pentane detections were made by the gas chromatograph. Pentane was not detected by the fiber optic sensor.

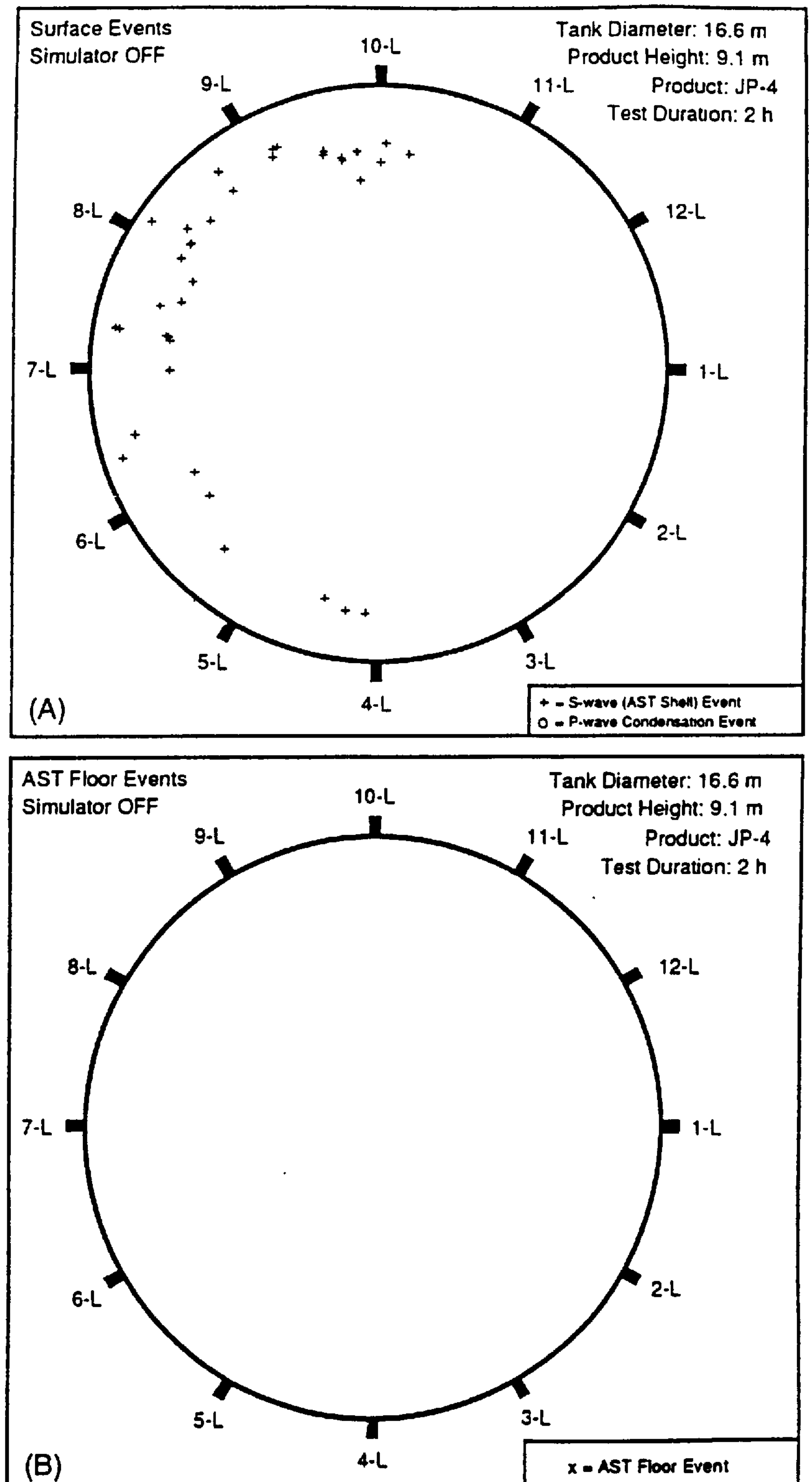

Figure 4-3. Acoustic events: (a) surface events (control tank, simulator OFF); (b)floor events (control tank, simulator OFF).

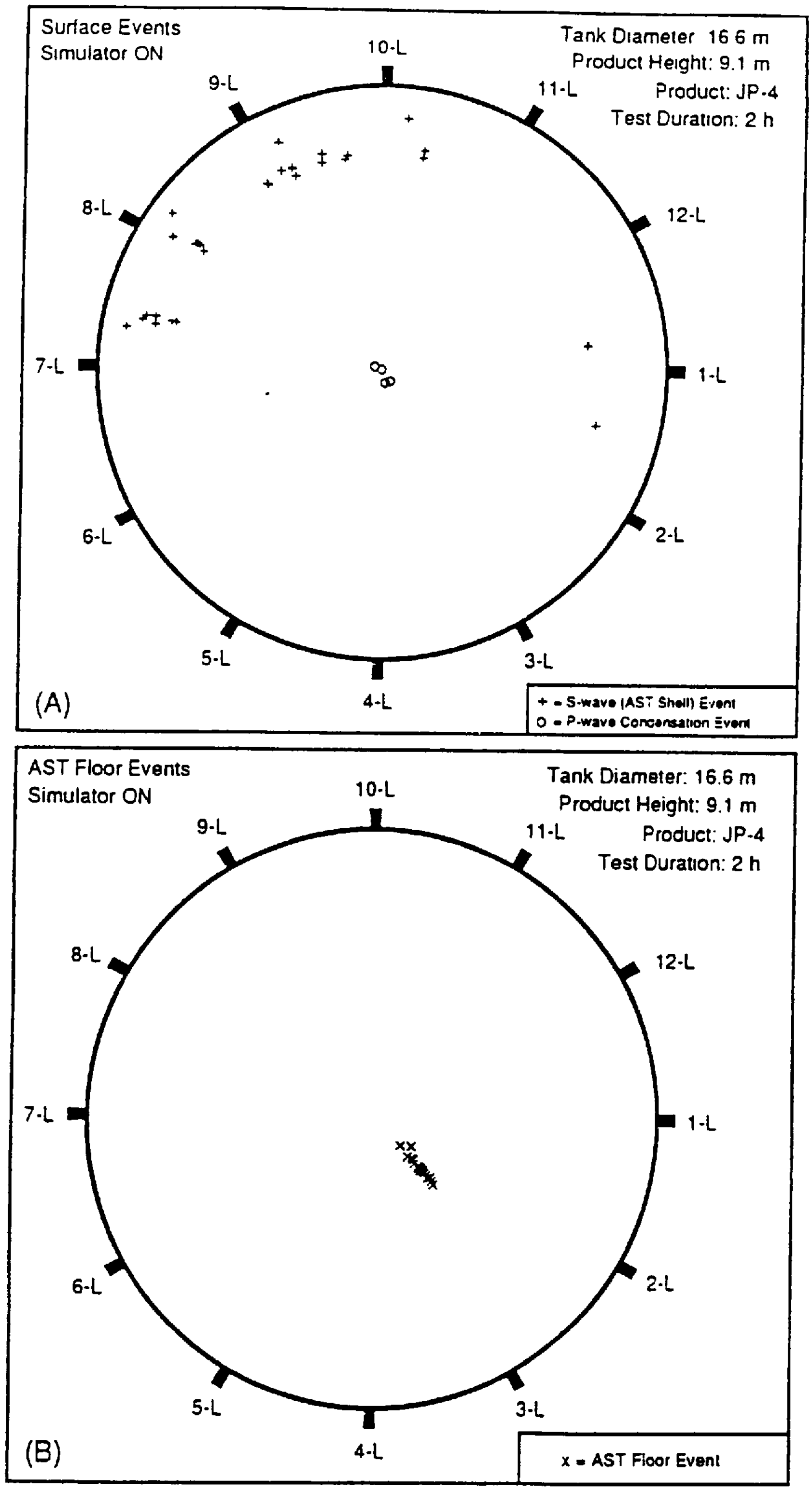

Figure 4-4. Acoustic events: (a) surface events (control tank, simulator ON); (b) floor events (control tank, simulator ON).

After the soil vapor tests had been completed, a high-product-level mass-measurement test was conducted. The results of this test were inconclusive due to the effect of floating-roof motion, which is discussed in Appendix B of this report.

LEAK DETECTION TESTS

Leak detection tests using the proposed methodology were conducted on the remaining 13 ASTs between 7 April and 3 May 1993. Acoustic and soil-vapor monitoring tests were conducted on all 13 tanks. The results of these tests are given in Table 4-2.

Table 4-2. Summary of Leak Detection Tests

	SOIL VAPOR MONITORING		PASSIVE ACOUSTIC				
Tank No.	No. of Wells	Result	Test Duration (h)	Total Number of Hits	Floor Hits	Hits Due to Conden-sation	Hits Due to Roof Motion
36	2	No measurable hydrocarbons	4	534	0	1	402
37	2	No measurable hydrocarbons	10	1136	0	0	762
22	3	No measurable hydrocarbons	10	866	0	3	802
2	2	No measurable hydrocarbons	6	743	0	262	368
9	2	No measurable hydrocarbons	6	564	0	17	265
7	2	No measurable hydrocarbons	6	100	0	33	44
3	2	No measurable hydrocarbons	5	532	0	81	338
24	2	No measurable hydrocarbons	4	580	0	70	437
18	2	No measurable hydrocarbons	4	599	0	0	474
19	2	No measurable hydrocarbons	4	653	0	0	449
15	2	No measurable hydrocarbons	4	1418	0	26	1260
14	2	No measurable hydrocarbons	5	1120	0	68	732
16	2	Less than 2 ppm pentane measured at both wells. No other hydrocarbon detected.	4	350	0	31	310

Six hours was allotted for the conduct of acoustic tests, two hours for setup and calibration and four hours for data collection. The period set aside for data collection was extended when additional time was available. Up to two tanks were tested each day. Product levels were at 80 to 90 percent of tank capacity. Acoustic testing was completed on schedule and, as mentioned earlier, did not in any case indicate the presence of a leak.

In the soil-vapor monitoring tests, where pentane was the tracer element, a gas chromatograph was used to sample the air beneath each of the tanks. Under most of the tanks, two monitoring wells each consisting of a ten-foot section of pipe were positioned at a 180° angle to one another. Under Tank 22, three monitoring wells were positioned radially at intervals of 120°. Unlike the control tests, no suction was applied to any of the monitoring wells. Under 12 of the 13 tanks, no pentane was detected; at the two monitoring wells under Tank 16, less than 2 ppm of pentane was detected. The presence of pentane under Tank 16, however, is not believed to have been caused by a leak. If product had been leaking into the backfill, several other constituents of that product would have been detected by the gas chromatograph. The detection of pentane is thought to have been caused by contamination of either the test sample or the equipment.

Volumetric tests performed on Tank 9 were 48 h in duration and were conducted with product level at 3 ft. As in the control test, level-and-temperature and mass-measurement data were collected concurrently from 20 to 22 April. Level-and-temperature measurements indicated an average outflow of 0.38 gal/h over the 48-h period, while mass measurements indicated a 1.5 gal/h inflow during the same period. The discrepancy between these two results is believed to be caused by uncompensated thermal effects on the mass-measurement test equipment. Level-and-temperature and mass-measurement data are shown in Figures 4-5 and 4-6, respectively. Four-hour mass balancing tests were conducted a number of times during the two days of testing on Tank 9. A large number of data sets were contaminated by the effects of direct solar heating of the differential pressure gauge. The data provided for analysis were collected between 0450h and 0835h on 22 April. During this period, two identical measurement systems were operating concurrently. Flow rates measured by the two systems during this period were -0.96 and +2.7 gal/h, respectively. The discrepancy between these two measurements cannot be explained on the basis of the available data. The two systems were mounted on the tank at different times and

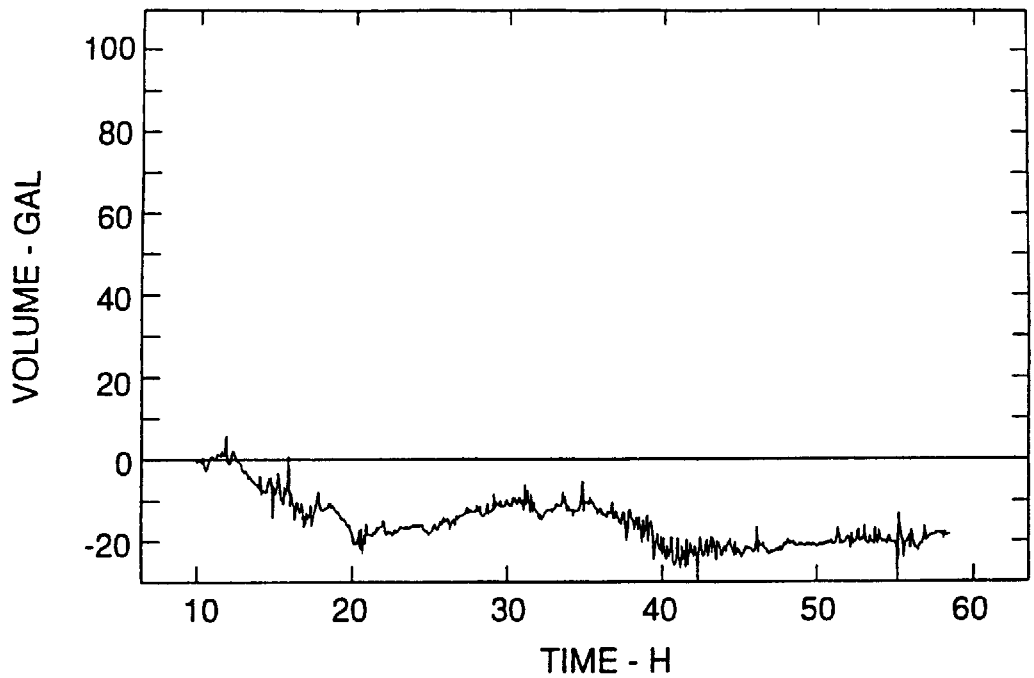

Figure 4-5. Level-and-temperature volumetric data (Tank 9).

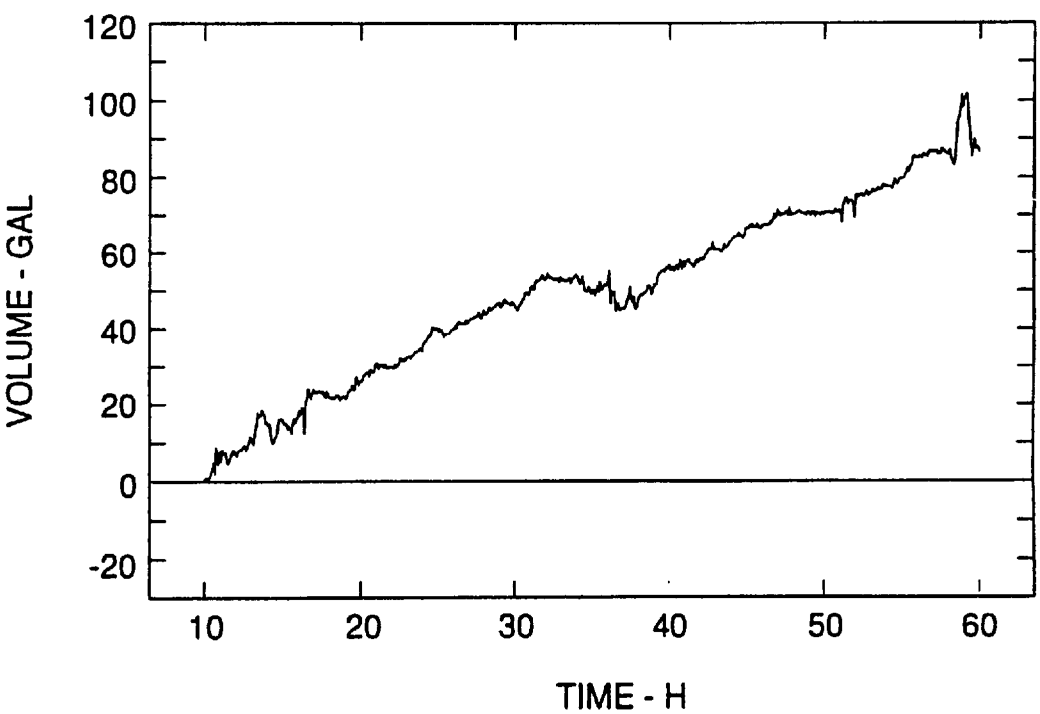

Figure 4-6. Mass-measurement volumetric data (Tank 9).

were therefore subject to different heating environments prior to the time that the measurements were made. The magnitude of the measured flow rates is consistent with known thermal effects on differential-pressure-measurement instrumentation.

Level-and-temperature data from Tank 2 were collected over a 48-h period from 1 to 3 May. During this time the roof of Tank 2 was floating on the product surface. High-product-level mass measurement tests were also conducted on this tank. These data were analyzed to assess the impact of the floating roof on test performance. The results of these analyses are given in Appendix B.

Section 5

CONCLUSIONS AND RECOMMENDATIONS

Based on the results of this test series, a number of conclusions can be drawn regarding the performance of each of the three technologies and of the overall test methodology. These conclusions are described below, with recommendations for future study in each area.

TEST METHODOLOGY

A testing methodology that uses multiple technologies will provide a robust test result. In order for such a methodology to be effective in improving the reliability of a test decision, two criteria must be met. First, the technologies included in the methodology must have acceptable performance in terms of probability of detection and probability of false alarm, and second, each of the technologies must be independent. If noise affects each technology in a different way, the performance of the *multiple-technology methodology* is enhanced. In this test series, independence was achieved in that sources of noise that affected the performance of one technology did not affect the others.

Because this test series did not result in any detections, the performance of the methodology cannot be evaluated directly. The performance of a methodology such as the one used in this program should be evaluated under circumstances in which one or more technologies indicate the presence of a leak. This can be accomplished in one of two ways: tests can be conducted on tanks that are suspected of leaking, or enough tests can be conducted on a tight tank that false alarms occur.

PASSIVE-ACOUSTIC TECHNOLOGY

The results of this test series indicate that passive-acoustic technology, as demonstrated in this program, can be employed on a wide range of tanks and still maintain a low probability of false alarm. Leak detection tests that use this technology differentiate acoustic signals from impulsive noise events primarily on the basis of the origin of the signal, i.e., its location. A detection is made when a number of acoustic events are located in an area on the tank floor that is consistent with the location accuracy of the acoustic sensor array. There are two sources of illusory events that can lead to false detections. One consists of acoustic signals that seem to originate on the AST floor but in reality do not. The other consists of impulsive acoustic signals that are generated at the AST floor but that are due to factors other than a leak. It was shown during the acoustic tests that the collection and analysis of digital time series reduced the number of false events due to the mislocation of impulsive acoustic noise. Acoustic tests performed in accordance with the methodology prescribed in Phase III of this program indicated *no false events in any of the tanks tested.* This is an extremely important finding given that false events can lead to erroneous test results. Erroneous results can occur in two ways: a concentration of false events in a pattern consistent with the location accuracy of the acoustic sensor array will be incorrectly identified as a leak (false alarm); a large number of false events can mask a grouping of true leak signals, so that a leaking tank will be incorrectly declared intact (missed detection). In addition, there were *no non-leak sources of impulsive acoustic signals originating from the floor* in any of the tanks tested. All of the tanks had internal, floor-mounted structures such as roof drains, pivoted float arms, or roof supports. It was thought that such structures might generate acoustic signals originating at the floor and thus be a source of false events. In none of the 14 tanks tested, however, were impulsive signals found to have originated from the tank floor.

Acoustic tests in which digital time series data were not used showed a large number of false events. Although these did not cause any false alarms, a concentration of false events in one tank indicated the need for a retest. These false events are believed to have been caused by the mislocation of impulsive noise generated at the product surface by the motion of the floating roof.

The two primary noise sources identified in this test series both originated at the product surface: condensate dripping onto the product surface and the motion of the floating roof. Acoustic noise sources were found to propagate through the product as pressure waves and through the tank shell as shear waves. Correct identification of the propagation mode for each signal received was critical to correctly locating all noise sources. It was found that incorrect identification of the propagation mode can lead to a grouping of false events which can be misidentified as a leak. As identified in Phase III, another potential source of false events caused by mislocation is the multipath reflections of acoustic signals within the tank (Vista Research, Inc., 1993a). These reflections, which were frequently larger than the direct-path signal, can cause a source of impulsive noise at the product surface to be mistakenly identified as a leak. The test and analysis approach demonstrated in Phase III, which involves the collection and analysis of time series data, was shown to be very effective in correctly identifying signal propagation and reflection characteristics; use of this approach resulted no false events over the course of the test series.

Persistent, non-impulsive noise from a nearby freeway and railroad yard was effectively reduced through analog filtering. Persistent noise can adversely affect acoustic leak detection tests by increasing the root mean square (rms) noise level against which the impulsive leak signal must be detected. Noise levels measured after analog filtering were sufficiently low to allow the reliable detection of leak signals of a magnitude consistent with those measured in Phase III.

Over the course of this program, many of the issues involved in passive-acoustic leak detection have been studied and are now better understood. A number of sources of impulsive, acoustic noise have been identified and characterized. The data collection and analysis approach implemented here has been shown to correctly differentiate these noise sources from the leak signal. The result is a test that has a low probability of false alarm and is applicable to a wide variety of tank configurations. Data collected during Phase III, on a tank with controlled leaks of known size and rate, indicate that the approach implemented here should also have a high probability of detection (Vista Research, Inc., 1993a). The remaining issue is the persistence of the impulsive leak signal under actual conditions. Further tests should be conducted on tanks with known or suspected leaks for the purpose of determining the characteristics of the impulsive leak signal and evaluating the detection performance of the passive-acoustic test method.

SOIL-VAPOR MONITORING TECHNOLOGY

During the control tests in which pentane was injected into a section of pipe under the AST, the rate of propagation of this gas through the oiled-sand backfill at the test site was too low for either the fiber-optic sensor or the gas chromatograph to detect a leak. In the interest of better understanding the propagation characteristics of pentane, additional injection tests were conducted at another site where the backfill material was sand that had not been oiled and was therefore much more porous. In this second series of tests, the injected pentane was reliably detected.

Soil-vapor monitoring techniques have potential for detecting leaks in ASTs; it is clear that in these tests, however, the effectiveness of the technology was severely limited by the low permeability of the oiled-sand backfill at the test site. The effect of a low-permeability backfill material in slowing the propagation of the target vapor can be mitigated through the use of a more stable substance as the target vapor and through the use of longer test durations. In order for this technology to achieve a reasonable probability of detection, the propagation characteristics of the target vapor through the backfill under a given tank must be well understood. Only then can the spacing of monitoring wells and the duration of the monitoring period be properly determined. The predictive capabilities required for reliable application of this technology must be developed and verified through additional work.

The existence of a layer of water at the bottom of the tank, although not experimentally investigated in this program, is known to prevent the release of product and therefore of pentane. Prior to this series of tests, water was drained from all tanks. No measurement of water level was made immediately before a leak detection test, however. Any water in the bottom of an AST can be a source of missed detections for pentane soil-vapor monitoring, and unevenness in the tank floor can make characterizing the thickness of any water layer very difficult. If a reasonable probability of detection is to be ensured, this issue must be addressed prior to conducting any test based on pentane soil-vapor monitoring.

VOLUMETRIC TECHNOLOGY

Two types of low-product-level volumetric tests were conducted, one based on level-and-temperature measurements and the other based on mass measurements. The performance achieved by both types of test is consistent with the findings in Phase III, in which 48-h tests were able to detect leaks of about 1 gal/h. Although the noise mechanisms that affect each type of test are different, the magnitude of error was similar in both cases.

In level-and-temperature tests, the primary source of noise is believed to be the horizontal gradients in the rate of change of temperature of the product. Evidence of this was seen in both of the level-and-temperature tests that were conducted. The phenomenon was similar to that observed in the Phase III tests (Vista Research, Inc., 1993b). A more complete characterization of product temperature would greatly enhance level-and-temperature system performance. Further experimentation is required, however. The extent of the instrumentation required to adequately characterize product temperature changes must be determined, and the mechanisms that cause or contribute to heating and cooling of product in an AST must be characterized. On the basis of this information, the horizontal and vertical spacing of thermistors can be determined analytically such that the desired performance is achieved.

Mass measurement tests were susceptible predominantly to thermal influences on the equipment, although expansion of the product and the tank shell also contributed some error. In addition to thermal expansion of the product below the measurement tube, the data showed evidence of the effects of thermally induced changes in the viscosity of the gas used in the bubbler tubes. Thermal effects on the differential pressure gauge are also thought to be a significant error source, based on previous experience. In the Phase IV test series the data were insufficient to quantify this effect.

Both mass-measurement and level-and-temperature data collected during Phase IV show that a leak detection test would be severely degraded by the effects of a floating roof resting on the product surface. In tests where this was the case, apparent changes in volume of 200 to 300 gal were measured over 3-h periods. These relatively abrupt changes in measured volume typically occurred when product temperature was near a local maximum or minimum. The apparent volume changes can be explained by a change in roof motion characteristics with respect to product expansion and contraction. As the rate of expansion or contraction of the product slows, the floating roof ceases to move freely with the product. The frictional forces acting on the roof seals cause the roof to stop moving before the product has stopped expanding or contracting. When the roof stops moving, product is forced to expand into the area around the edge of the roof, and into roof openings. Since this area represents only about ten percent of the total surface area of the tank, level changes in the tank are 10 times greater when the roof stops moving than when the roof is free-floating. In addition, external forces such as wind and rain can dramatically affect the way in which the roof floats on the product surface. It was evident from the data collected in this test series that roof motion can be a significant source of noise, and one which can preclude accurate test results.

The two high-product-level volumetric tests were both conducted on floating-roof tanks while the roof was floating on the product surface. In both tests, the tank was subject to the extreme apparent volume fluctuations described above. Because the effects of the floating roof were dominant in these data sets, the effect of the high product level on test performance could not be evaluated.

Data collected during this test series indicate, as did tests in Phases II and III, that when a volumetric test is less than 24 h long -- i.e., shorter than one diurnal cycle -- it is subject to large errors related to temperature fluctuations. In tests less than 24 h long, the signal generated by a leak emanating at a constant rate of flow cannot be differentiated from cyclic thermal influences.

Section 6

IMPORTANT TEST FEATURES

A number of conclusions can be drawn from the API AST leak detection program. Conclusions drawn from all four phases of this work have been organized here into a summary of the key features of each of the leak detection techniques studied.

PASSIVE-ACOUSTIC TECHNOLOGY

If it is to find leaks in the floor of an AST, a passive-acoustic system should be designed to detect the impulsive signal generated by such leaks. Off-the-shelf, frequency-selective sensors that are available commercially appear to be more than adequate for this purpose. For high performance, however, it is necessary to formulate data collection and signal processing algorithms that will detect this type of signal. The general features of such data collection and processing techniques have been derived from the results of the Phase II, III, and IV field tests and analyses.

- **Digital time series.** Digital time series of the raw acoustic waveform from each sensor must be collected and made available for analysis. Without digital data, the analysis required for robust leak detection cannot be performed. Although it would be desirable to collect continuous time histories, this would not be practical since the quantity of data collected during a normal test is prohibitively large. Continuous time histories are not essential provided that each time series is sufficiently long to correctly identify the leading edge of the direct-path signal in the presence of multiple events, multipath reflections, and impulsive acoustic noise. The data acquisition process should record a time series which is at least six tank diameters in duration (i.e., the time required for an acoustic signal propagating through the product to travel a distance equal to six times the diameter of the tank). The time series should include a minimum of four tank diameters prior to the data-acquisition trigger event, and two tank diameters after the trigger event.

- **High data collection threshold.** A high threshold is the best way to detect the impulsive acoustic signal produced by a leak and to minimize false alarm due to noise fluctuations. A high threshold is practical in acoustic testing due to the high signal-to-noise ratio (SNR) associated with this method.

- **Multipath discrimination.** The strongest acoustic returns tend to be multipath signals, a fact that confuses most conventional analysis algorithms. A critical requirement for high performance, therefore, is the implementation of an algorithm that distinguishes multipath reflections from the direct-path signal.

- **Time registration of events.** The algorithm must be implemented in such a way that the impulsive returns from discrete bubble events are isolated and that the direct-path signals are properly time registered.

- **Sensor spacing.** Close sensor spacing improves the system's ability to properly time-register bubble events and to discriminate between direct-path and multipath signals. However, as the aperture of the sensor array decreases, so does the accuracy of the leak location estimates. The optimal sensor configuration should address both accurate location estimates and proper registration of impulsive events. In order to discriminate between signals originating at the floor of the AST and those originating at the product surface, the array must include at least one sensor that is separated from the others in the vertical plane.

- **Averaging.** Methods of appropriately averaging the data are needed as a way to reduce the noise and enhance the signal. In both data collection and data analysis, the approach should be to select high-quality events and average them.

- **Propagation velocity.** The speed at which the acoustic signal propagates through the product in the tank must be known, as well as the speed with which it propagates through the tank shell. This acoustic propagation velocity can be measured at the time of testing.

SOIL-VAPOR MONITORING TECHNOLOGY

Tests conducted at several different sites indicate that the soil-vapor monitoring method is capable of detecting small leaks in ASTs provided that the test is properly conducted and that certain conditions are satisfied. The features that should be considered in the design of a leak detection system (and accompanying test protocol) based on soil-vapor monitoring technology include the following.

- **Backfill.** Sampling wells are used to monitor the backfill under the AST for vapor. The number of wells required for a given tank is a function of (a) the tank diameter, (b) the decay time of the target vapor, and (c) the diffusive characteristics of the backfill. Some backfills provide a poor environment for the diffusion of target vapors from the leak site to the sensor wells. It is essential that backfill conditions beneath the AST be understood in order to estimate the system performance under a particular set of testing conditions.

- **Water Layer.** Due to environmental conditions (rainfall, condensation, etc.), there is a layer of water at the bottom of many ASTs. If a water layer is present in a leaking tank, and if the target vapor does not penetrate water, the concentration of this vapor in the backfill will be diminished. In order for soil vapor monitoring techniques to achieve optimal performance, the substance selected as a target vapor should be one that will penetrate water, or the test protocol should specify that the water layer must be removed. The time that must elapse between the removal of the water layer and the beginning of a test will depend on the diameter of the AST and on the diffusive characteristics of the backfill.

- **Background Level.** To ensure that background concentrations of the target vapor will be low, and that any vapor released as a result of a leak will be easily detected, the substance selected as a target vapor should be unique. It is recommended that background levels of the target vapor in the vicinity of the AST be assessed through sampling as part of the test protocol.

VOLUMETRIC TECHNOLOGY

The features of a volumetric test that are crucial to high performance have been identified. The design of a volumetric test must carefully address the diurnal fluctuations observed in the volume data that are controlled by the ambient air temperature (Vista Research, Inc., 1991; Vista Research, Inc., 1993b). Important design considerations common to both types of volumetric leak detection system (those based on level-and-temperature measurements and those based on mass measurements) are listed first. They are followed by design considerations unique to one approach or the other.

It should be noted that either type of volumetric technique can be implemented with commercially available measurement systems.

- **Waiting Period.** Before the start of a test, it is recommended that a waiting period of at least 24 h be observed, during which time no product is added to or removed from the tank. This allows inhomogeneities in the product to dissipate (level-and-temperature systems will be affected by thermal inhomogeneities, while mass measurement systems will be affected by inhomogeneities in product density) and any deformation of the tank shell to subside. (The waiting period is an established part of the protocol for testing USTs; because of the continuous nature of the data in the experiments described here, the duration of the waiting period was not verified independently as part of the current work.)

- **Low Product Level.** The product level should be low enough to optimize the signal-to-noise ratio. Good performance was achieved when the product level was at approximately 3 ft. This minimized the overall thermally induced volume changes and resulted in nighttime horizontal gradients that were small enough to be negligible.

- **Long Test Duration.** The duration of the data-collection period during a volumetric leak detection test should be at least 24 h and preferably 48 h. Test durations that are whole multiples of a diurnal cycle should be used unless it is demonstrated that a slightly longer or shorter duration will yield better temperature compensation. This would be the case if, for example, differences in temperature (whether of the ambient air, the shell, or the product) were less over a period of 22 or 26 h than over the full 24 h.

- **Test at Night.** For best performance, a test should begin and end at night when there are no large changes in ambient air temperature and no uneven solar heating of the tank perimeter. Testing at night is equally important to both measurement approaches, since both are affected by expansion of the tank shell and by evaporation and condensation. There are also different reasons for testing at night that are particular to each approach. The fact that horizontal gradients in the rate of change of product temperature are sufficiently small at night means that a level-and-temperature system is a viable tool in leak detection; and the fact that the rate of change of the ambient air temperature is constant at night permits more accurate compensation of the thermally sensitive differential pressure sensor used in a mass-measurement system.

- **Digital Data Collection/Sampling Rate.** The data should be collected digitally, so that the benefits of a variety of the more complex noise cancellation and data analysis algorithms can be realized. A sampling interval between 1 and 10 min is recommended.

- **External Temperature Sensors.** As a means of compensating for thermally induced changes in the tank shell, an array of six external temperature sensors is recommended. These should be mounted on the steel outer wall and around the perimeter of the AST; they should be shaded from direct sunlight. When the data processing algorithm uses only the data from the beginning and end of a test initiated at night, fewer temperature sensors may suffice.

- **Known Coefficient of Thermal Expansion and Known Height-to-Volume Conversion Factor.** The coefficients required for temperature compensation and for conversion of level or mass changes to volume changes should be known beforehand or should be measured as part of the test. A different set of constants will be required for each measurement approach. Errors in these constants will produce a bias in the test results that might be large enough to suggest the presence of a leak. In addition, the height-to-volume conversion factor must remain constant during the test. Structures floating on the product surface can cause dramatic variations in the height-to-volume ratio over the course of a test and will induce significant errors in the test result.

- **Sufficient Instrumentation Precision.** The combined precision of the level-and-temperature instrumentation used to measure the rate of change of the thermally compensated volume, regardless of approach, must be sufficient to sense a leak approximately one-third the size of the smallest leak to be detected reliably. A low-precision level sensor, for example, can be improved by increasing the test time. A method for estimating the minimum duration of a test conducted with level and temperature sensors that have a given precision is discussed in (Vista Research, Inc., 1993b).

- **Compensation for Thermally Induced Volume Changes.** All thermally induced volume fluctuations need to be compensated for. In all instances, they can be minimized by means of a long test. Because the leak signal does not have a diurnal period, any diurnal fluctuations remaining in the compensated volume data are indicative of an error.

Additional features that are important for high performance and that are particular to level-and-temperature measurement systems are listed below.

- In order to minimize sensor motion due to thermal expansion and contraction of the sensor mounting structure, the sensors should be mounted on a stand at the bottom of the tank rather than suspended from the top or attached to the sides of the tank.

- An array of horizontally and vertically spaced temperature sensors with the best precision available (typically 0.001°C) is required in order that thermally induced changes in the product can be compensated for. The vertical spacing of the temperature sensors should be no greater than 8 in.; since most of the temperature changes occur in the upper portion of the product, and strong gradients are present in the lower portion, it is recommended that sensors be spaced more densely in the upper and lower layers of product (e.g., every 4 in.). Further study is required before the maximum horizontal sensor spacing can be determined.

- The coefficient of thermal expansion of the product and steel shell, the volume of product in the tank, and the height-to-volume conversion factor must be known before a test is conducted. The coefficient of thermal expansion should be experimentally determined as part of the test procedure.

Additional features that are important for high performance and that are particular to mass-measurement systems are listed below.

- The thermal sensitivity of the instrumentation must be minimized as part of the setup. It is essential that all tubes used to connect the differential pressure (DP) sensor to the tank be horizontal and that all trapped air be completely removed from the tubes and the sensor. Additional temperature sensors attached to the body of the DP sensor and to the connecting tubes might be required in order to compensate for changes in ambient air temperature. Since it was not possible to develop a compensation algorithm during the course of this analysis that could be universally applied to all of the differential pressure data, it cannot be stated with certainty that additional thermal problems will not occur when the pressure connections are made with horizontal tubes. The data obtained from a system configured with horizontal tubes suggest that thermal fluctuations still persist, even after thermal compensation (Vista Research, Inc., 1993b).

- The coefficient of thermal expansion of the steel shell, the specific gravity of the product, and the height-to-volume conversion factor are required. If an accurate experimental estimate of the height-to-volume conversion factor is made during a test, then the specific gravity does not have to be known.

- Pressure measurements should be made as close to the tank bottom as possible. When measurements made more than a few inches from the bottom of the tank, the expansion and contraction of the product below the measurement point must be accounted for; i.e., the temperature of the product must be characterized and thermal changes must be compensated for.

REFERENCES

Vista Research, Inc. 1991. *An Engineering Assessment of Volumetric Methods of Leak Detection for Aboveground Storage Tanks*. API Publication Number 306. American Petroleum Institute. Washington, D.C.

Vista Research, Inc. 1992. *An Engineering Assessment of Acoustic Methods of Leak Detection in Aboveground Storage Tanks*. API Publication Number 307. American Petroleum Institute. Washington, D.C.

Vista Research, Inc. 1993a. *An Engineering Evaluation of Acoustic Methods of Leak Detection in Aboveground Storage Tanks*. API Publication Number 322. American Petroleum Institute. Washington, D.C.

Vista Research, Inc. 1993b. *An Engineering Evaluation of Volumetric Methods of Leak Detection for Aboveground Storage Tanks*. API Publication Number 323. American Petroleum Institute. Washington, D.C.

Appendix A

THE ACOUSTIC NOISE ENVIRONMENT ASSOCIATED WITH ABOVEGROUND STORAGE TANKS

Eric G. Eckert, Michael R. Fierro, and Joseph W. Maresca, Jr.
Vista Research, Inc.
Mountain View, California

ABSTRACT

Experiments were performed on operational, non-leaking aboveground storage tanks (ASTs) in order to assess the effect of acoustic noise on a passive-acoustic leak detection system. Leak tests of at least four hours' duration were conducted on both fixed-roof and floating-roof ASTs containing a variety of light petroleum products. The results of the experiment showed that several forms of impulsive acoustic noise may increase the probability of false alarm associated with a leak test. Noise sources observed included condensate dripping onto the air/product interface, slippage between the floating roof and the AST shell, noise transmitted from nearby ASTs as a result of filling and dispensing operations, and several forms of persistent noise such as vehicle traffic and wind.

Impulsive noise that originated from the AST shell was observed to propagate as both compressional waves through the product and as shear waves through the AST shell. Localized sources of impulsive noise that propagated through the shell were mapped into the AST interior as a result of the application of a location algorithm designed to locate leak signals. Time series of the acoustic signals were required in order to identify the propagation mode of impulsive noise. Multi-path propagation associated with both compressional and shear waves was observed. The majority of impulsive noise was emitted above the AST floor. The ability to discriminate between floor and surface acoustic events is shown to be critical with regard to the elimination of false alarms. Several forms of persistent noise external to the AST (primarily wind and pump noise) were observed to couple to sources of impulsive noise.

INTRODUCTION

Passive-acoustic (or *acoustic emission*) leak detection methods have been applied to the problem of detecting small leaks in the floor of an aboveground storage tank (AST). While it is important that a leak detection system utilizing acoustic measurements exhibit a high probability of detection (P_D) when operated under a broad range of test conditions, the cost and operational impact of internal tank inspections requires that the probability of false alarm (P_{FA}) be minimized. Since the manner in which noise is handled by the detection system largely determines the P_{FA}, it is important to observe the response of a leak detection system during tests in which *no leaks* are present.

Passive-acoustic leak detection systems operate primarily on the principle of *detection through location.* An AST is determined to be leaking if acoustic signals consistent with signals produced by leaks are emitted from one or more locations on the tank floor. Additional information such as the strength, duration, propagation mode, and spectral character of the leak signals may be used to reject data that are contaminated by ambient noise. The results of laboratory simulations and field experiments have shown that only the large-amplitude, impulsive component of the acoustic leak signal can be exploited for the purpose of leak detection (Eckert and Maresca, 1991, 1993; Miller, 1990; Nickolaus, 1988, 1989; Nordstrom, 1990). By measuring the arrival time of impulsive leak signals at spatially-separated elements of a sensor array, the origin of each event can be estimated through application of a simple least-squares location algorithm (Eckert and Maresca, 1991; Nickolaus, 1988). The output of a typical acoustic leak detection test presently consists of a *location map* on which the measured location of each acoustic event originating from the AST floor is plotted.

The dominant feature of location maps resulting from acoustic leak detection tests is often a random distribution of location estimates on the AST floor (Miller, 1990; Nickolaus, 1989). Such a distribution of events clearly indicates the influence of some form of noise on the conduct of the tests. The noise contamination raises a fundamental question regarding acoustic leak detection: Is the detection system correctly responding to numerous sources of impulsive acoustic noise distributed over the entire AST floor, or is the output of the detection system degraded by improper processing of localized impulsive noise? Previous acoustic leak detection studies include modest attempts to characterize the acoustic noise associated with ASTs (Eckert and Maresca, 1993; Miller, 1990; Nickolaus, 1989). However, since most published work concerns fixed-roof ASTs, and because time series of the acoustic signals are not recorded as part of most leak tests, the description of the acoustic noise environment is incomplete.

This work describes the results of a series of acoustic leak detection tests conducted on 13 operational, non-leaking ASTs during April 1993. Both fixed-roof and floating-roof ASTs containing a variety of light petroleum products were tested as part of the experimental program. The data described in this work were originally obtained as part of a three-method effort to assess the integrity of the 13 ASTs. Leak detection tests based upon mass measurement, soil vapor monitoring and passive-acoustic techniques indicated that none of the ASTs was leaking. Given that leaks were not present in any of the tested tanks, the focus of the acoustic measurements was shifted toward a detailed analysis of the noise sources typically encountered during an acoustic leak test. Details of the spatial origin and propagation modes of acoustic noise are understood through analysis of time series. In addition, location maps are presented in order to show the effect of various noise sources on the output of the detection system.

The results of the acoustic noise characterization experiment may be summarized as follows:

- Localized sources of impulsive acoustic noise were frequently observed during the conduct of the leak detection tests.
- No impulsive acoustic noise was observed to originate from any portion of the AST floor.
- The majority of impulsive acoustic noise originated from the AST shell as a result of slippage between the floating roof and the tank shell, and from the product surface as a result of condensation.
- Acoustic noise was observed to propagate both as compressional waves (P waves) through the product and as shear waves (S waves) through the AST shell.
- Multi-path signals caused by the reflective interior of the AST were frequently observed to exceed the direct-path signals in amplitude.
- Systematic errors in the processing of impulsive acoustic noise may significantly increase the probability of false alarm associated with a leak detection test.
- The direct effects of persistent, non-impulsive acoustic noise were successfully eliminated through filtering of the analog signals. However, coupling between some forms of persistent and impulsive noise suggests that recording in the audio frequency range could reduce false alarms.

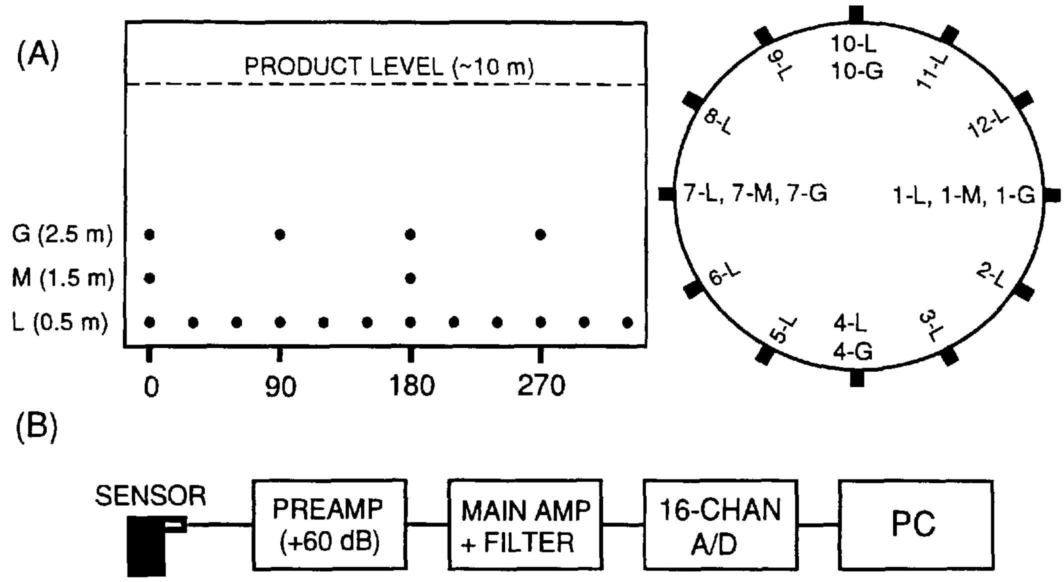

Figure 1. (A) Diagram of the sensor array used in the experiment. Location (L) and Guard (G) sensors are PAC A-3s; Monitor (M) sensors are CTI-30s. (B) Diagram of the data acquisition system. The external trigger is designed to initiate data acquisition when a signal exceeding a preset threshold level is detected.

EXPERIMENT DESIGN

The ASTs tested during the experiment ranged from 54 to 73 ft in diameter. Two of the tanks were of fixed-roof construction while the remainder utilized floating roofs to control product loss via evaporation. The backfill beneath each tank consisted of oiled sand. Prior to the acoustic leak tests, sampling tubes were inserted beneath each of the ASTs as part of the soil-vapor monitoring leak test. The time between the sampling tube installation and the conduct of the acoustic leak test ranged from 1 day to 2 weeks. Due to consistent high winds encountered during daytime hours, the majority of the 4-h acoustic leak tests were performed between 2200h and 0600h. Sources of persistent acoustic noise included wind, auto and rail traffic, warning sirens used at the AST terminal, and pump noise associated with dispensing operations from nearby tanks. Each leak test was conducted at a product level within 20% of the AST capacity.

Figure 1 shows a diagram of the sensor array and data acquisition system used in the acoustic leak tests. The sensor array used to locate the source of acoustic signals consisted of 12 elements spaced at 30° intervals around the AST circumference. The vertical position of each location element was 0.5 m above the AST floor. In order to discriminate between floor and surface acoustic events, guard sensors were installed 2.0 m above the location sensors at the 0°,

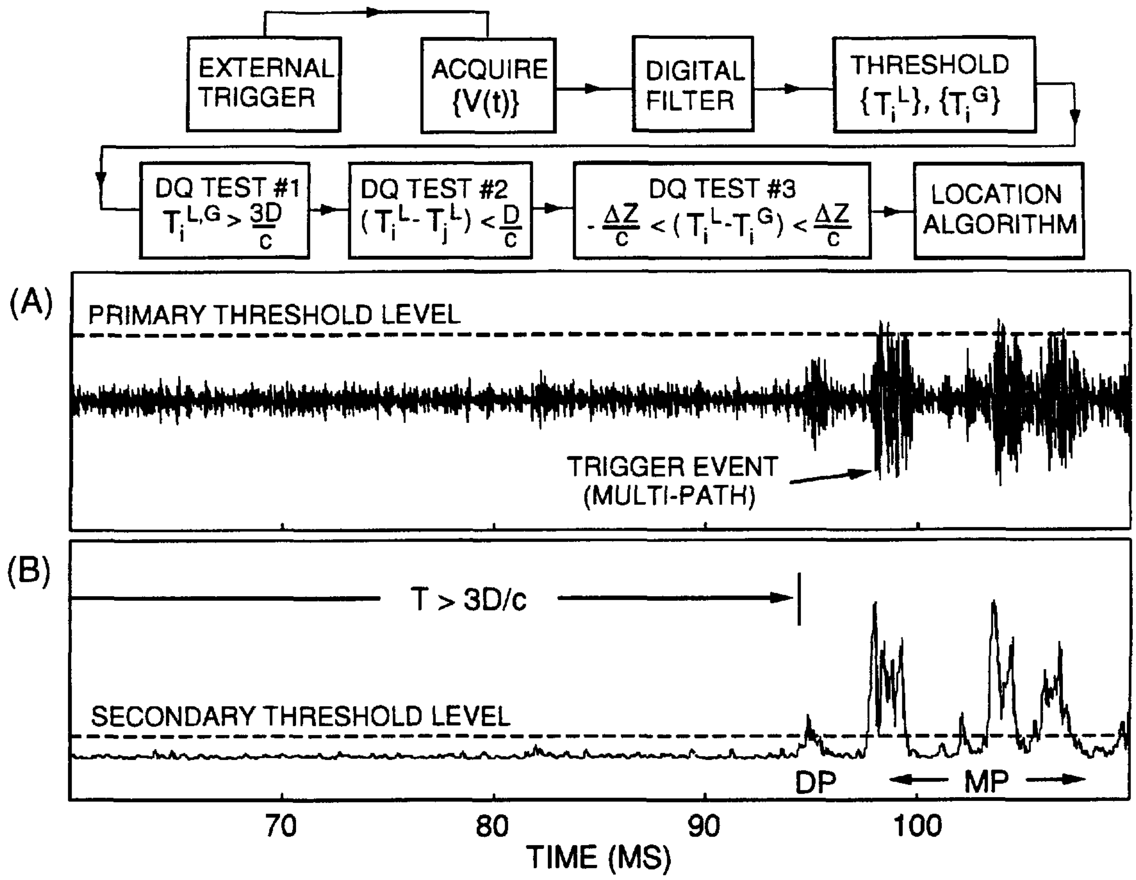

Figure 2. The signal processing strategy. Time series of pressure fluctuations (A) are converted to time series of fluctuations of received power normalized to the power standard deviation (B). Arrival times of the impulsive signal at each element of the sensor array (T_i) are obtained by application of a low-level secondary threshold. Sets of arrival times, $\{T_i\}$, that pass a series of data quality tests are processed by a simple least-squares location algorithm. The superscripts L and G denote location and guard array elements; c is the speed of sound in the product; Δz is the vertical separation between L and G array elements.

90°, 180°, and 270° positions. The 12 location and 4 guard sensors were Physical Acoustics A-3, 30-kHz resonant piezoelectric sensors whose outputs were amplified and highpass-filtered by a Physical Acoustics Spartan AE System. Two CTI-30 piezoelectric sensors were installed 1.0 m above the location sensors at the 0° and 180° positions. The CTI-30 transducers were used to monitor ambient acoustic noise within the audio-frequency band (DC-20 kHz). Panametrics 5660-C preamplifiers and Krohn-Hite 3342 amplifying anti-alias filters were used to condition the CTI-30 signals. Simultaneous, 131-ms-duration realizations of the acoustic signal received by each of the 16 sensor channels were digitized by an STI Flash-12 data acquisition card operating at a sampling frequency of 62.5 kHz.

Figure 2 illustrates the signal processing strategy used to analyze time series of the acoustic signal. Since the impulsive leak signal occurs infrequently and can be large in comparison to the persistent noise level, data acquisition is initiated by the reception of a trigger signal that exceeds a preset primary threshold level. The primary threshold levels used in the experiment ranged between 5 and 30 times the rms noise level and resulted in the sampling of between 50 and 200 acoustic events per hour. The position of the trigger event within the time series was set such that 100 ms of data preceded the trigger. In order to estimate the spatial origin of acoustic events, the arrival times of the impulsive signal at each element of the sensor array must be measured. The impulse arrival times are measured by applying a low-level, secondary threshold to the time series for each sensor. Impulsive events are enhanced relative to the persistent ambient noise by application of a digital filter that measures fluctuations in received power normalized to the power standard deviation. The secondary threshold is set low enough to discriminate between the direct-path and reflection signals (Eckert and Maresca, 1993), and high enough to be unaffected by fluctuations in the persistent noise. Prior to application of the location algorithm, each set of impulse arrival times is subjected to three data quality tests. First, the threshold exceedance must occur at least 3D/c beyond the start of each time series, where D is the AST diameter and c is the speed of sound in the product. This test increases the chance that the measured impulse corresponds to the reception of a direct-path (i.e., source-to-sensor) signal, and does not represent an artifact of reverberation within the AST. Second, it is required that the difference in arrival time between impulsive signals received by each pair of sensors be less than D/c. Finally, a comparison between vertically spaced array elements (e.g., 1-L and 1-G) must clearly indicate whether the signal was emitted from above or below the location array. Sets of impulse arrival times which pass these data quality tests are processed by a simple least-squares location algorithm in order to estimate the source location. Since acoustic leak signals have been shown to propagate primarily through the product (Eckert and Maresca, 1991, 1993), the location algorithm assumes that all signals propagate along straight lines through the product at the product wave speed ($\sim$ 1250 m/s). The ensemble of source locations resulting from a leak test are plotted as a set of markers on a map of the AST floor. In addition to estimating the source location of each event, the rms signal strength for each element of the sensor array is computed. The raw time series collected during the course of a leak test are saved for post processing. A typical 4-h leak test results in between 100 and 250 MBytes of archived data. The ability of the acoustic leak detection system to identify a localized source of impulsive signals was verified during a series of control tests performed on a 55-ft-diameter AST containing 32 ft of JP-4. A remotely operated bubbler immersed at several locations within the tank was easily located.

SOURCES OF IMPULSIVE NOISE

The use of externally mounted transducers in passive-acoustic leak detection systems complicates the process whereby sources of impulsive signals are located. External sensors respond primarily to two modes of wave propagation: compressional waves in the product (P waves), and transverse waves in the AST shell (S waves). Typical measured wave speeds of the P and S propagation modes for a gasoline-filled, steel AST were 1250 m/s, and 2200 m/s, respectively. In addition to variations in propagation speed among the two modes, the paths along which S waves propagate from source to sensor are geometrically dissimilar from the paths followed by acoustic waves in the product. Another complication introduced by external sensors is the fact that multi-path reflection signals are generally strongest for sensors on or near the AST shell (Eckert and Maresca, 1993). The accurate location of a source of impulsive signals can be obtained only if the propagation mode of the signal is known. The propagation mode can be identified only through the inspection of time series of the impulsive signal.

Figure 3 shows the result of a 4-h acoustic leak test conducted on a 54.5-ft-diameter AST of floating-roof construction. The acoustic noise level associated with sources external to the AST was very low during the test, and the measured wind speed was less than 5 mph. Markers on the plot indicate the (x,y) position of acoustic sources; the marker type indicates the source mechanism. The bold line in the plot shows the result of a ray-tracing simulation that will be discussed below. Of 600 impulsive events processed by the location algorithm, this figure shows the 200 events for which the least-squares error in location estimate is the smallest. Several features of the noise environment encountered during acoustic leak tests are exhibited in this plot. First, no acoustic events were observed to originate from the AST floor. This is somewhat surprising since (a) the tank had been filled to a level of 33 ft 24 h prior to the test, and (b) the backfill beneath the AST had been drilled at several locations in order to insert sampling tubes for the soil vapor monitoring test. Second, the majority of source locations

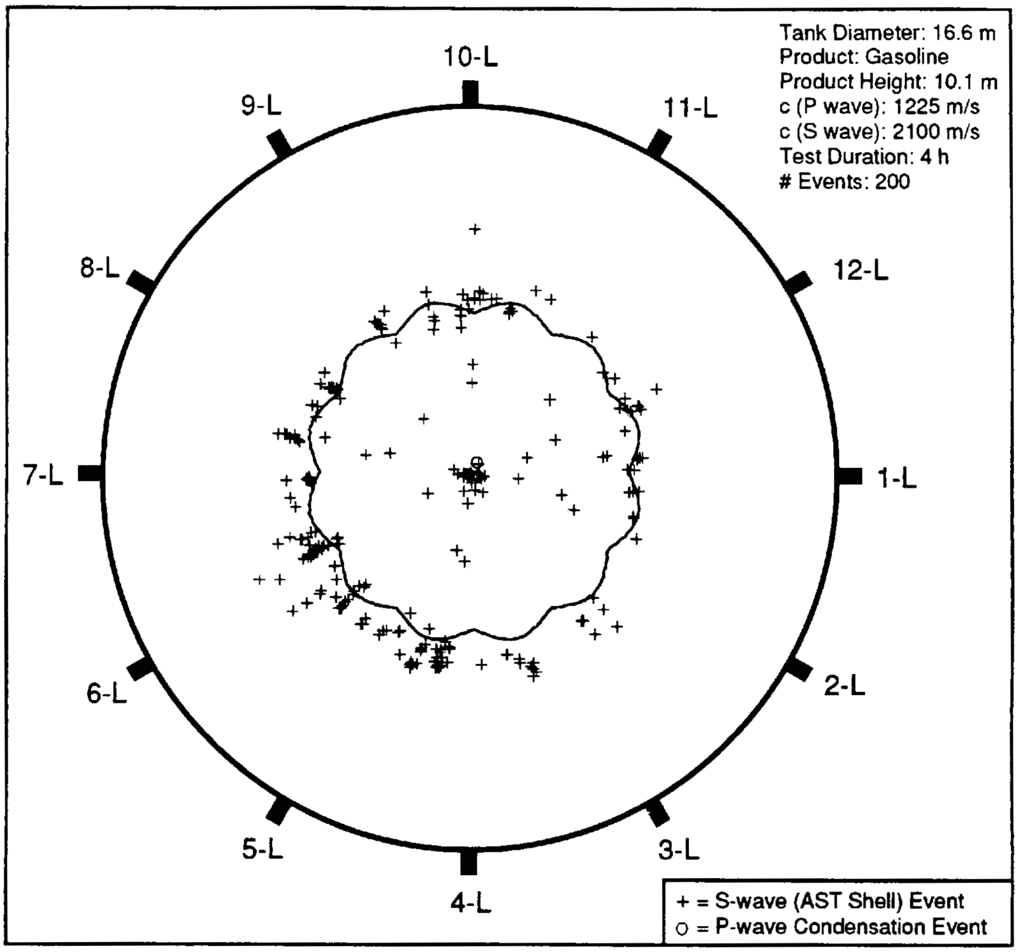

Figure 3. Location estimates resulting from a 4-h acoustic leak test. No impulsive events were observed to originate from the AST floor. The solid line shows the expected image of the floating-roof perimeter obtained by processing simulated S-wave impulses with the P-wave location algorithm.

clearly define a ring whose diameter is less than the diameter of the AST. Finally, a cluster of source locations lies near the center of the AST. The ring image is caused by the emission of impulsive noise during slippage between the floating roof and the AST shell. This noise often propagates as S waves, and so is improperly processed by the leak signal (P wave) location algorithm. The diameter of the ring image depends on the ratio of the S-wave and P-wave propagation speeds and on the ratio of product height to tank diameter.

Figure 4 shows time series of the signal received as a result of the localized slippage between the floating roof and the AST shell. The bold lines in Figure 4 indicate the expected arrival time of an S wave emitted at the floating-roof perimeter based upon a simple ray-tracing simulation in which the wave speed was set to the measured S-wave value (2100 m/s) and the propagation was along straight paths through the AST shell. Multi-path propagation caused by

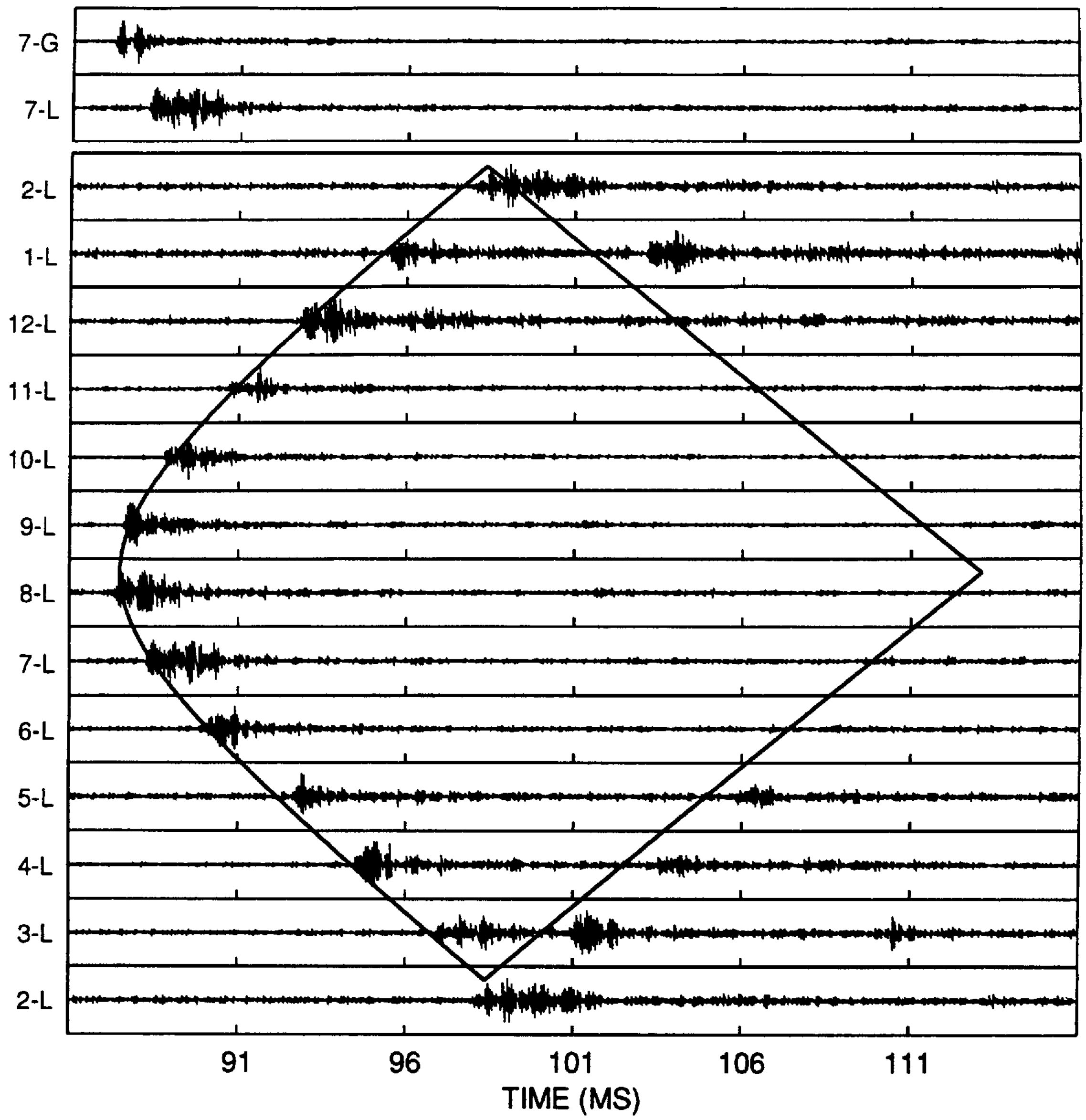

Figure 4. Time series of the acoustic signal produced by slippage between the floating roof and AST shell. Solid lines indicate the expected arrival times of an S-wave impulse at the array elements assuming that the propagation is through the AST shell at c=2100 m/s. The multi-path signal (trailing solid line) results from propagation in two directions around the AST. Sensor pair 7-L and 7-G clearly show that the signal originates from above the location array.

S waves traveling in both clockwise and anticlockwise directions around the AST shell is also evident at several of the sensor locations. Inspection of the time series corresponding to the vertically separated sensor pairs (7-L and 7-G) indicates that the source of the impulsive signal lies above the AST floor. The frequency of impulsive noise emission was observed to increase dramatically during periods of high winds. However, in the absence of wind, the noise source was still present, suggesting that thermal changes may play a role in exciting slippage between the floating roof and AST shell. The cluster of source locations near the tank center is caused by slippage events in which a large portion of the floating-roof perimeter moves over a short time scale ($\leq$ 5 ms). These events are characterized by large-amplitude, long-duration signals that arrive at the location sensors at approximately the same time.

Further evidence that impulsive noise emitted from the floating-roof perimeter is mapped into the AST interior by acoustic leak detection systems is provided by application of the P-wave location algorithm to an ensemble of simulated S-wave impulses. The bold line shown in Figure 3 is the theoretical image of the circular floating roof computed by emitting 500 simulated S-wave impulses at equally spaced points around the floating-roof perimeter. The tank diameter, product height, and propagation speeds used in the simulation were the same as the measured values used to estimate source locations of actual impulsive noise events.

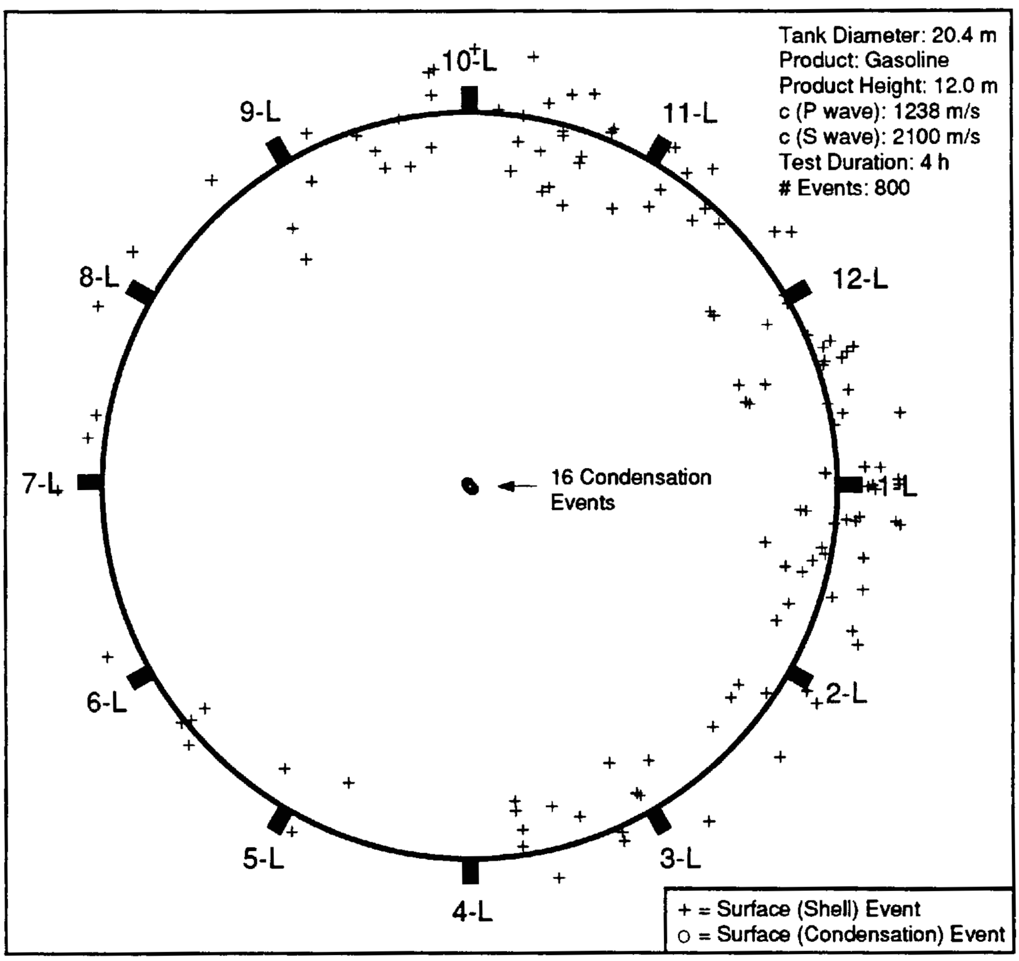

Figure 5. Location estimates resulting from a 4-h acoustic leak test. No impulsive events were observed to originate from the AST floor. The impulsive noise caused by floating-roof slippage propagates to the sensor array in the form of P waves. The location of the condensation events corresponds to a 6-in. access on the AST roof.

Several ASTs were observed to emit impulsive noise from the floating-roof perimeter in the form of P waves propagating through the product. Figure 5 shows the results of a 4-h acoustic leak test conducted on a 67-ft-diameter AST of floating-roof construction. The diameter of the image of the floating-roof perimeter in Figure 5 is approximately equal to the actual AST diameter. Evidence that this type of impulsive noise propagates through the product can be seen in the time series of Figure 6. The bold lines in Figure 6 indicate the expected arrival times of the direct-path and two multi-path signals propagated from the floating-roof perimeter through the product to the location array. The paths traversed by the simulated multi-path signals of Figure 6 are source-wall-sensor (MP1) and source-floor-surface-sensor (MP2). It should be noted that (a) several of the array elements receive multi-path signals that exceed the direct-path signal in amplitude, and (b) the two sensors closest to the source (11-L and 10-L) exhibit the weakest response to the signal. The reason that the roof/shell slippage mechanism results in S-wave propagation in some ASTs and P-wave propagation in others appears to be due to differences in the floating-roof's interface with the AST shell. In certain types of floating roofs, the connecting gasket between the roof and AST shell may be in contact with the product, while in others this interface may lie above the product level.

The cluster of location estimates near the center of the AST shown in Figure 5 are caused by condensate dripping at an access port near the center of the AST. While such drips were observed over the entire product surface in fixed-roof ASTs, the drip locations were confined to the center access port in floating-roof ASTs. Figure 7 shows time series of the acoustic signal produced by condensate dripping near the center of a 73-ft-diameter AST. Only four location sensors and their vertically spaced guard sensors are shown in the plot. Two observations should be noted regarding this measurement. First, the relative arrival times of the multi-path and direct-path signals are consistent with reflections of the acoustic signal from the AST floor. Second, the direct-path signal is consistently smaller in amplitude than the multi-path signal. If a threshold is applied to the time series of Figure 7 to determine the impulse arrival time, it is likely that three out of the four sensor pairs shown would incorrectly indicate a source originating from the AST floor. Since, for floating-roof ASTs, the condensation noise source is highly localized, an error in processing that maps this noise onto the AST floor must be recognized as a possible source of false alarms.

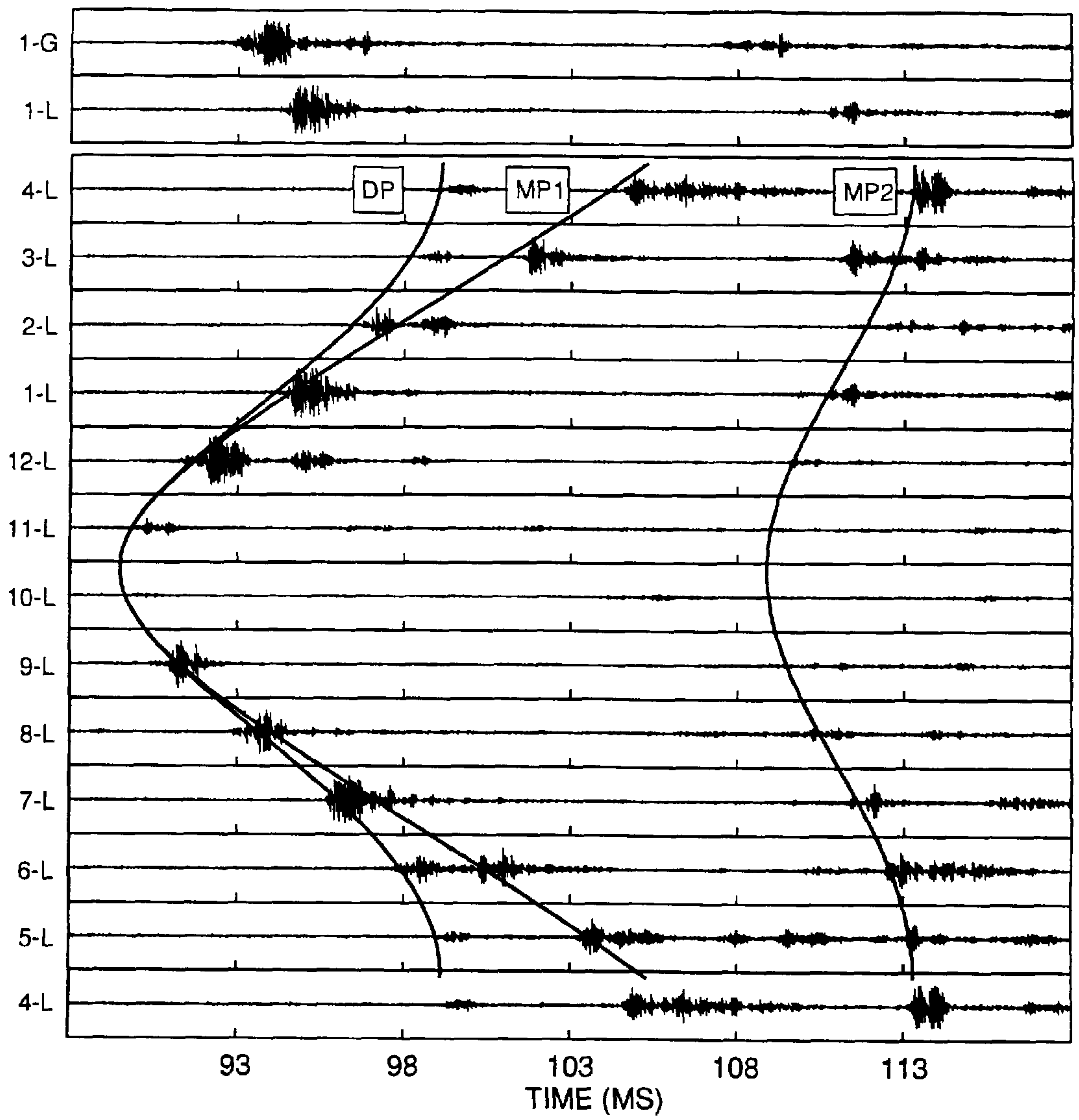

Figure 6. Time series of the acoustic signal produced by slippage between the floating roof and AST shell. Solid lines indicate the expected arrival times of a P-wave impulse at the array elements assuming that the propagation is through the product at c=1238 m/s (the measured wave speed). Sensor pair 1-L and 1-G clearly show that the signal originates from above the location array.

Fixed-roof ASTs provide an acoustic environment that is generally much quieter than the noise field associated with floating-roof tanks. Figure 8 shows the results of a 7-h acoustic leak test performed on a 70-ft-diameter, fixed-roof AST. Of the 100 noise events recorded during the test, location estimates for the 34 events whose error in location is the smallest are shown on the plot. Events located on the product surface were all observed to propagate as P waves. The localized source on the surface near the AST wall is believed to be associated with the automatic tank gauge. This particular test resulted in the only evidence of any sources on the

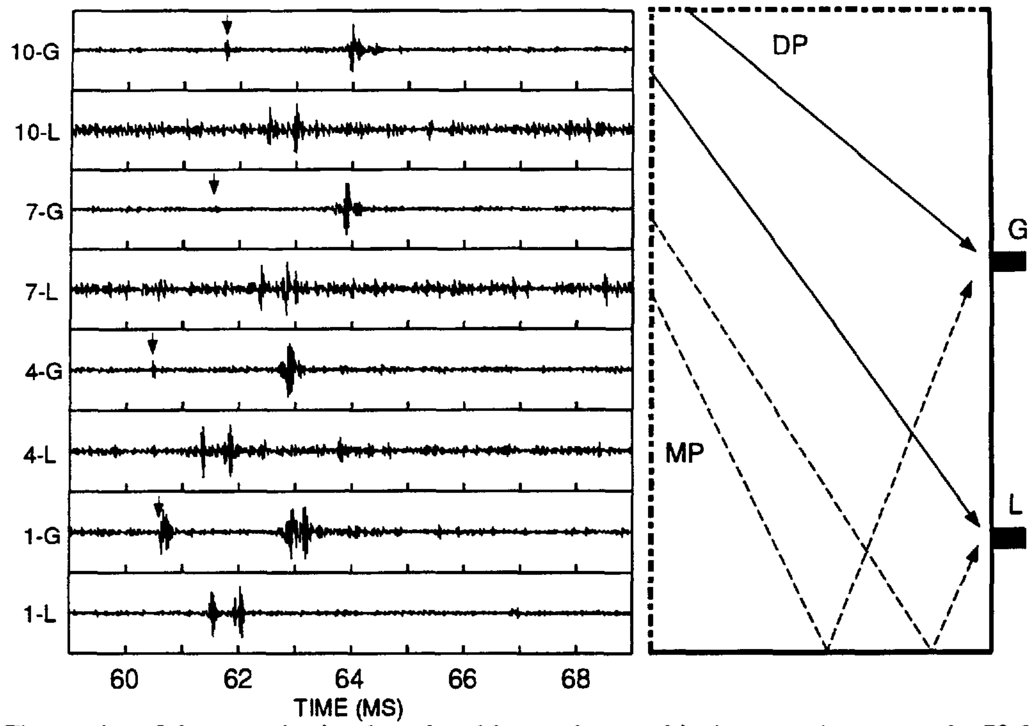

Figure 7. Time series of the acoustic signal produced by condensate dripping near the center of a 73-ft-diameter AST. Arrows indicate the direct-path (source-to-sensor) signal as measured by the guard sensors. The propagation paths for direct- and multi-path signals are illustrated by the diagram. Note that three of four guard sensors receive a direct-path signal that is small in comparison to the multi-path signal.

AST floor. The localized source mapped onto the AST floor in Figure 8, however, is not believed to be caused by a leak. Figure 9 shows time series of a noise event recorded by the location-guard sensor pair (1-L, 1-G) and the CTI-30 broadband sensor (1-M). The difference in impulse arrival time between sensors 1-L and 1-G clearly indicates that the source of noise is located below the midpoint between the two sensors. Inspection of the time series for each element of the location array indicates that the event shown in Figure 9 represents S-wave propagation. Thus, it is apparent that the event originated *on* the AST shell. Due to the relatively high P-wave propagation speed (~ 1450 m/s for diesel fuel), the source is mapped only a small distance into the AST interior as a result of the P-wave location algorithm. Had the wave speed been assumed to be that of gasoline (~ 1200 m/s), the source location would have been mapped to a point approximately midway between the AST's center and its edge. An interesting feature of this time series is the ringing response of the broadband sensor at a frequency of approximately 2.5 kHz. The noise source observed during this test is believed to be either a wire intermittently slapping the AST shell, or a mechanical disturbance associated with the automatic tank gauge (ATG).

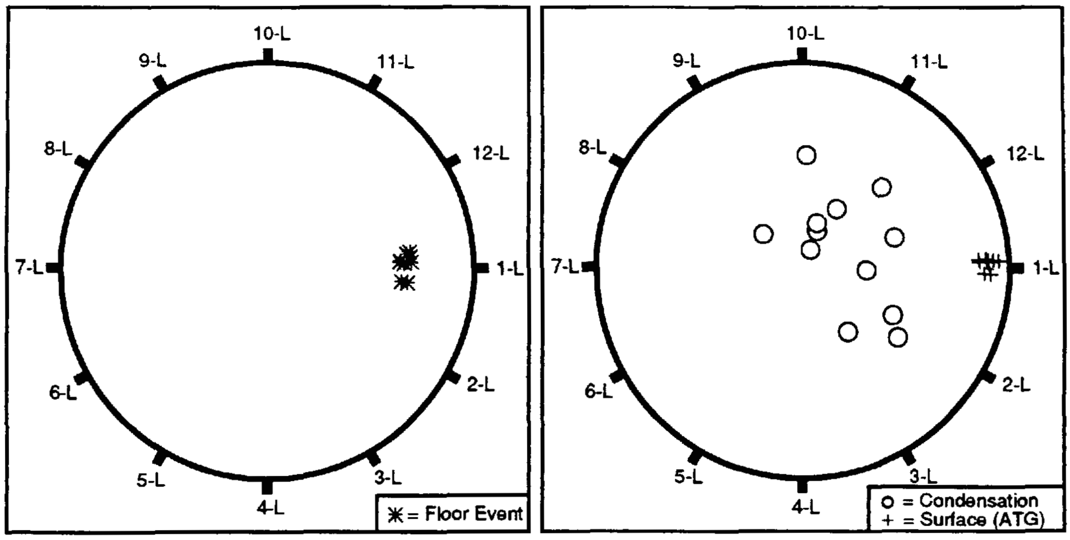

Figure 8. Location estimates resulting from a 4-h acoustic leak test. Floor events originate from the AST shell near the ATG; propagation mode of floor events is S-wave. The AST diameter is 21.3 m; product height is 9.6 m. Product is diesel with a measured P-wave speed of 1450 m/s.

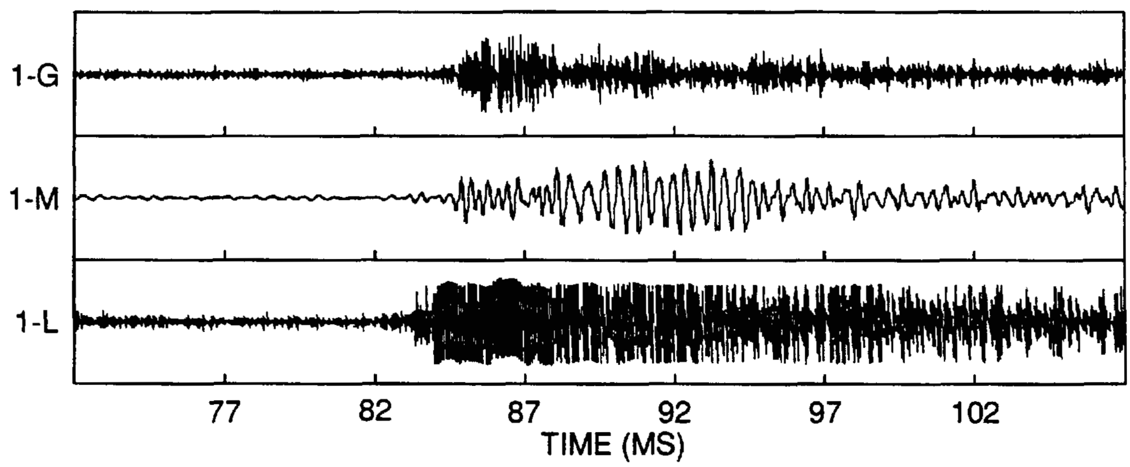

Figure 9. Time series of a floor event recorded by the location-guard pair 1-L and 1-G, and by the broadband monitor sensor 1-M. Arrival times for the entire location array and the shell excitation recorded by 1-M suggest an S-wave noise source caused by an impulsive force applied to the AST shell.

THE PERSISTENT NOISE ENVIRONMENT

In the context of acoustic leak detection, persistent acoustic noise is defined as sound that is present during all measurement periods. Sources of persistent noise typically encountered during the acoustic leak detection experiments included traffic (both auto and rail), wind, and pump and flow noise transmitted to the AST through connecting pipelines as a result of dispensing operations from nearby tanks. While these types of noise sources are termed persistent, significant variations in the strength of the noise can be observed over time scales

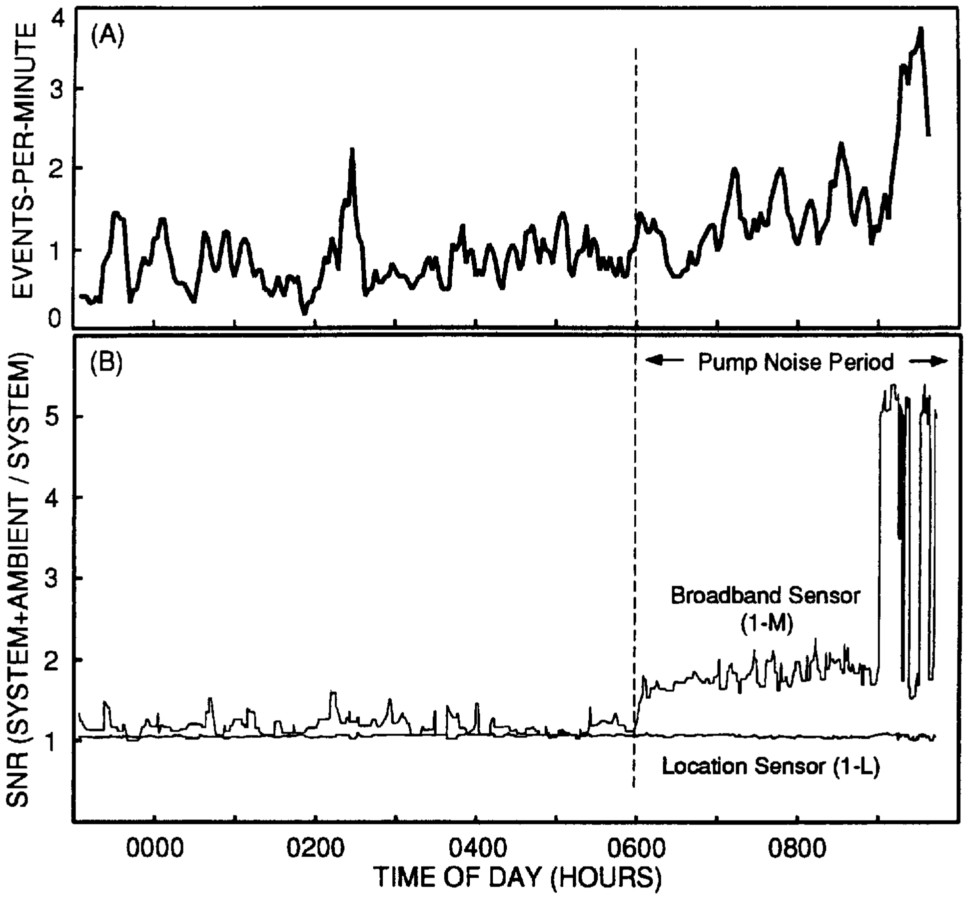

Figure 10. (A) Time series of the average number of impulsive events recorded per minute during an 11-h acoustic leak detection test. (B) Time series of SNR measured by a broadband monitoring sensor (1-M) and a highpass-filtered, location sensor (1-L) during the experiment.

ranging from a few seconds to many hours (Eckert and Maresca, 1993; Nordstrom, 1990). Persistent noise adversely affects acoustic leak tests by increasing the rms noise level against which the impulsive leak signal must be detected and, more importantly, by exciting sources of impulsive noise that must be collected and processed by the detection system. Examples of the latter effect include floating-roof impulses excited by wind stress against the AST and impulsive noise associated with the operation of pumps and valves. Since the impulsive leak signal is broadband in character and persistent noise is largely concentrated in the audio frequency band (Eckert and Maresca, 1993), the primary means of avoiding persistent noise is to apply a highpass filter with a cutoff frequency of between 15 kHz and 30 kHz to the analog output of each sensor channel prior to digitization of the signal. While this technique virtually eliminates the direct effect of persistent noise, it can also discard useful information concerning the probable origin of recorded impulsive events.

The coupling between impulsive and persistent noise sources was investigated through the conduct of an 11-hour leak test on a 54.5-ft-diameter AST of floating-roof construction. During this test, signals from two of the guard sensors (4-G and 10-G) were discarded and instead two broadband CTI-30 channels (1-M and 7-M) were recorded. Figure 10-b shows the signal-to-noise ratio (SNR) for location sensor 1-L, whose output was highpass filtered, and the broadband sensor 1-M, set to respond primarily to signals in the audio band (DC-20 kHz). Figure 10-a displays the average number of recorded impulsive events per unit time. The SNR is computed by dividing the rms signal level of the ambient noise plus system noise by the rms level of the system noise. The abrupt rise in SNR recorded by the broadband sensor at approximately 0600h is caused by pump noise associated with filling operations at a nearby tank. During the period of elevated persistent noise level (0600h to 1000h), the location sensor showed no increase in SNR. Thus, as far as processing impulsive signals is concerned, high levels of persistent noise will not degrade the system's ability to locate a source. However, inspection of the events-per-minute plot (Figure 10-a) shows that an increase in impulsive noise level accompanied the rise in persistent noise. Without the extra information provided by the broadband sensor, the impulsive events recorded during the period of elevated persistent noise level may have been attributed to sources located within the AST. Many sources of noise that influence acoustic leak testing are detectable by the ear alone, and so may be avoided through careful scheduling of the test. However, other sources (such as sounds confined to pipelines) may be subtle enough to require an additional broadband sensor affixed to the AST shell.

DISCUSSION

It has been shown through experiments conducted on non-leaking ASTs that a variety of sources of impulsive noise may be encountered during the course of a typical acoustic leak test. The similarity in character between these noise events and the signals produced by leaks, combined with the fact that impulsive noise is often localized, suggests that mishandling of noise may significantly increase the probability of false alarm associated with an acoustic leak detection system. Minimization of the false alarm rate can be accomplished by (a) the collection of long time series for some, if not all, of the acoustic events, (b) designing a robust means by which the vertical location of impulsive events is determined, and (c) employing at least one audio-range sensor as part of the monitoring transducer array.

The collection of time series of impulsive signals is required in order to properly handle multi-path propagation. The multi-path problem, which for impulsive leak signals is dominated by P waves, is compounded in the case of impulsive noise that can propagate both as P and S waves. The identification of S-wave emission is particularly critical since the locations of these sources are mapped from the AST shell into the AST interior, i.e., into the space in which leaks are confined. Most of the impulsive noise sources measured during the experiment were located near the air/product interface (for fixed-roof ASTs) or at the level of the floating roof. The collection of time series in which data acquisition was triggered by a relatively large threshold exceedance allowed surface events to be easily recognized. It should be noted, however, that (a) multi-path propagation can effectively reverse the sequence of impulse arrivals at vertically separated array elements (see Figure 7), and (b) as the primary threshold is lowered, the chance that a surface event will be misinterpreted as a floor event is increased. Since the majority of surface noise is localized, these errors can cause a source of impulsive noise above the AST floor to be mistakenly identified as a possible leak.

While it is important that the detection system correctly discriminate between surface and floor events, it is equally important that the location algorithm produce accurate estimates of the source location in the horizontal plane. The wide-aperture array of sensors employed in the field experiments minimizes errors in location caused by uncertainty in the arrival time of individual impulses. However, when array elements are positioned around the entire AST circumference, errors in location estimate caused by mixing direct-path and multi-path arrival times are more likely to occur. The time series of Figures 4 and 6 show that multi-path contamination is most severe for transducers that are far from the impulsive source. Improved location ability may result from application of the location algorithm to impulse arrival times supplied by a subset of the sensor array close to the source.

It is important to monitor low-frequency acoustic signals (DC-20 kHz) during the course of an AST leak test. During the experimental program, audio-band sensors were used primarily to monitor the persistent noise environment external to the AST and as an aid in tracking down sources of impulsive noise on the AST shell. Given that shell noise can be mapped into the

AST interior through the incorrect processing of S-wave events, the ability to merely listen to the sounds within the tank during the course of a leak test may significantly reduce the probability of false alarm.

Results presented in (Eckert and Maresca, 1993) and in this work suggest a simple way to view the multi-path propagation problem in AST leak detection. Multi-path propagation of leak signals, caused by reflections within the AST interior, maps acoustic energy from the tank floor to points located outside the AST. Leak detection systems that do not effectively handle multi-path propagation of leak signals will suffer a reduction in the probability of detection. Conversely, multi-path propagation of impulsive noise, caused by the excitation of S waves in the AST shell, maps acoustic noise into the interior of the tank. Detection systems that cannot discriminate between P-wave and S-wave events will thus be subject to an increase in the probability of false alarm.

It should be emphasized that acoustic leak detection tests of 13 operational ASTs resulted in no detectable impulsive noise sources on the floor of any AST. This result demonstrates the ability of an acoustic detection system to achieve good performance in terms of the probability of false alarm. Given that the typical AST floor is acoustically quiet, test results (i.e., location maps processed to include only floor sources) that contain large numbers of randomly distributed hits, or maps that exhibit artifacts of the floating-roof images shown in Figures 3 and 5, may indicate the need for more robust data collection and signal processing techniques.

REFERENCES

Eckert, E. G., and J. W. Maresca, Jr. 1991. Detection of Leaks in the Floor of Aboveground Storage Tanks by Means of a Passive Acoustic Sensing System. *Air and Waste Management Association.* 91.15.5.

Eckert, E. G., and J. W. Maresca, Jr. 1993. The Acoustic Signal Produced by a Leak in the Floor of an Aboveground Storage Tank. *Air and Waste Management Association.* A952.

Miller, R. K. 1990. Tank Bottom Leak Detection in Above-Ground Storage Tanks by Using Acoustic Emission. *Materials Evaluation.* 48(6):822-829.

Nickolaus, C. M. 1988. Acoustic Emission Monitoring of Aboveground Storage Tanks. *Materials Evaluation.* 46(3):508-512.

Nickolaus, C. M. 1989. Study of Acoustic Emission Signals Generated by Simulated Leaks in an Above Ground Storage Tank. Mobil Oil Corporation and Hartford Steam Boiler Inspection Technologies. 89RD02.

Nordstrom, R. 1990. Direct Tank Bottom Leak Monitoring with Acoustic Emission. *Materials Evaluation.* 48(2):251-254.

Appendix B

EXPERIMENTAL EVALUATION OF VOLUMETRIC METHODS OF LEAK DETECTION IN ABOVEGROUND STORAGE TANKS

Michael R. Fierro, Eric G. Eckert, and Joseph W. Maresca, Jr.
Vista Research, Inc.
Mountain View, California

ABSTRACT

The effects of noise on two methods of volumetric leak detection (mass-measurement-based and level-temperature-based) were studied through tests on three aboveground storage tanks. Although the specific noise mechanisms affecting each type of test are different, the noise in both cases is driven by ambient temperature changes. Both tests had approximately equal levels of performance. Good performance in either type of test requires accurate temperature compensation and a test duration longer than 24 h.

Limitations in the performance of the level-temperature-based volumetric test were due to inadequate characterization of product temperature changes during the test. The performance of this test can be improved through the use of a more extensive array of temperature sensors. The array must incorporate both horizontal and vertical elements, as opposed to the single vertical array used in the series of tests described here.

The performance of the mass-measurement-based volumetric test is believed to have been limited by incomplete thermal control of the testing equipment and incomplete thermal compensation for the effects of temperature on this equipment. In this series of tests, insulation and refrigeration were used in an attempt to control the effects of temperature. The mass-measurement-based volumetric test can realize performance improvements through the use of additional temperature compensation schemes.

The performance of both types of volumetric test was degraded by the effects of a floating roof resting on the product surface. Frictional forces acting on the roof caused noise that induced measurement errors. The noise, which manifested itself as apparent changes in the volume of product, makes volumetric testing impractical under these conditions (i.e., when the tank's floating roof is resting on the product surface).

INTRODUCTION

This work describes the results of volumetric tests performed on three ASTs during the period from March to May 1993. The data included in this report were originally obtained as part of a three-month effort to assess the integrity of 13 ASTs using a three-step, multiple-technology leak detection methodology. Leak detection tests based upon passive-acoustic and soil-vapor monitoring techniques were also conducted on the three ASTs for which volumetric data are given here. Based on the results of all tests conducted, none of the three ASTs is believed to be leaking.

For purposes of discussion, the volumetric tests conducted as part of this program have been divided into three types: (1) level and temperature, (2) mass measurement, and (3) mass balancing. Level and temperature measurements were made, respectively, with a float-based level sensor and thermistor arrays. Mass measurement tests used a differential-pressure-measurement device to determine the pressure in the product near the bottom of the tank; this measurement was referenced to atmospheric pressure. The mass balancing tests used the same kind of device, and for the same purpose; in this case, however, the measurement was referenced to the pressure at the bottom of a column of product outside the tank.

Level-and-temperature and mass measurement tests were conducted according to the protocols validated in previous phases of this program, which call for low product levels and a test duration of at least 24 h (Vista Research, Inc., 1991; Vista Research, Inc., 1993). Additional mass measurement tests were conducted in which a high product level was used. The mass balancing tests that were conducted used a low product level, but their duration (approximately 4 h) was significantly less than the recommended 24 h.

Data analysis focused on the sources of noise that affect the accuracy of each type of volumetric test. The results are presented in this paper, which includes, for each type of test, recommendations that will improve the reliability of the test decision.

EXPERIMENTS

The first volumetric test conducted in this program was a test on a control tank that was known, *a priori*, ***not*** to be leaking. This tank had just undergone an internal inspection that included dye penetrant, ultra-sonic, and magnetic flux inspection procedures. The second tank selected for testing (Tank 9) was chosen arbitrarily from the tank population. Passive-acoustic and soil-vapor monitoring tests conducted on this tank prior to the volumetric test indicated that it was not leaking. A third tank (Tank 2) was also selected for the conduct of a volumetric test. For safety reasons, however, site personnel required that the floating roof remain on the product surface, a condition that precluded the conduct of a reliable volumetric leak detection test. Volumetric data were nonetheless collected on this tank, and the impact of the floating roof was quantified. A description of the three tanks is given in Table 1.

The control tank and Tank 9 underwent level and temperature measurements made at low product levels and lasting 72 and 48 h, respectively; these were done according to the protocol validated in the Phase III API field tests. Tank 2 underwent measurements over a 48-h period, during which its roof was floating on the product surface.

Table B-1. Description of the Tanks Used in the Evaluation

	Control Tank	Tank 9	Tank 2
Diameter	54 ft 6 in.	60 ft 0 in.	73 ft 4 in.
Height	44 ft 10 in.	39 ft 3 in.	36 ft 8 in.
Roof Type	Floating Roof (Pontoon Type)	Fixed Cone Roof	Floating Roof (Double Deck)
Foundation	Oiled Sand	Oiled Sand	Oiled Sand
Product	JP-4	Turbine	Unleaded Regular
Expansion Coefficient of the Product	0.001035 in./°C	0.000864 in./°C	0.00125 in./°C

Mass measurement tests were conducted on all three tanks. In the control tank and Tank 9, mass measurements at low product level were made concurrently with, and had the same duration as, the level-and-temperature measurements. Mass measurements at high product level were made on the control tank and Tank 2.

Low-product-level mass balancing tests, conducted on Tank 9 over a 4-h period, employed a differential pressure sensor that was connected through hot taps installed in the side of the tank specifically for these tests. The low-product-level mass balancing tests were conducted concurrently with the other low-product-level volumetric tests on the same tank.

To prevent a loss of product from poorly sealed valves, the three tanks that underwent testing had valve blinds installed on all connecting pipelines.

THE LEVEL-AND-TEMPERATURE EXPERIMENT

Level measurements were made with a float-based level sensor that had a high degree of precision (0.0005 in.); it was supported by a tripod assembly that rested on the bottom of the tank. Temperature measurements were made with multiple arrays of precision thermistors that monitored the temperature of both the product and tank shell. Like the level sensor, the single vertical array of thermistors that characterized product temperature was mounted on a tripod assembly that rested on the tank floor. Mounting the sensors this way, rather than suspending them from above, reduces the effects of thermal expansion and contraction of the tank shell and of the mounting structure itself, and this is critical in achieving measurement accuracy. The six thermistors that characterized the temperature of the tank shell were mounted in a single horizontal array on the exterior of the tank. These were spaced at 60-degree intervals around the tank, at a height above the tank floor that was equal to approximately half the height of the product. The specific arrangement of these sensors varied slightly on each of the three tanks tested, as shown in Figure 1 a, b, and c.

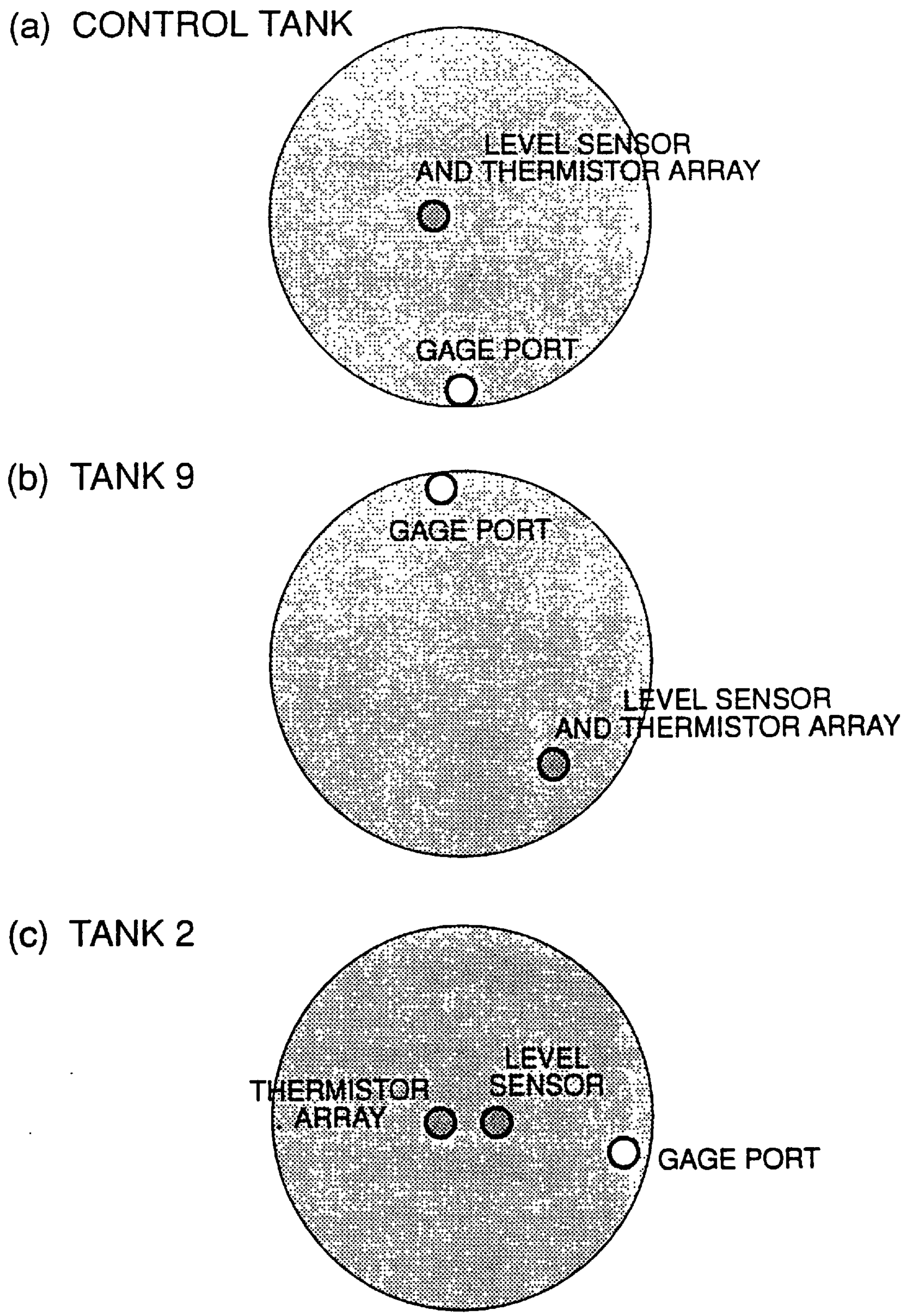

Figure 1. Location of sensors on the control tank (a), Tank 9 (b) and Tank 2 (c).

It has been shown that the greatest source of noise in level-and-temperature measurement systems is the thermal expansion and contraction of the product (Vista Research, Inc., 1993). As a means of compensating for this thermal expansion and contraction, the product was for analytical purposes divided into six horizontal layers, each centered on a thermistor in the vertical array, with the thickness of each layer determined by the spacing between thermistors. Each thermistor measured temperature at a different depth of product. The rate of change of temperature in each of the layers was assumed to be uniform. Based on this assumption, the expected change in the total volume of the product due to thermal expansion and contraction was calculated by summing the volume changes in each of the layers as follows:

$$\Delta TV = \sum_{i=0}^{n} C_{ep} V_{pi} \Delta T_{pi}$$

where

ΔTV	=	total thermal volume change
C_{ep}	=	coefficient of thermal expansion of the product
V_{pi}	=	volume of *i*th layer of product
ΔT_{pi}	=	change in product temperature in *i*th layer
n	=	total number of product layers
i	=	layer number

In addition to thermal expansion of the product, the effects of thermal expansion of the tank shell were also considered. Expansion and contraction of the tank walls change the capacity of the tank and therefore the level of the product in the tank. The six wall-mounted thermistors were used to record the temperature of the tank shell in order to compensate for this effect. In the data analysis, the tank shell was treated as the frustum of a cone; it was assumed that at floor level the diameter was fixed but that at the product surface it varied with temperature. The effect of this type of expansion and contraction on the level of the product in the tank was then calculated using the following expression:

$$\Delta TV_{sh} = \frac{h}{12\pi}((C_o + C_o \alpha \Delta T)^2 - C_o^2)7.4801$$

where

ΔTV_{sh} = apparent volume change due to shell expansion

C_o = shell circumference

α = coefficient of thermal expansion of the shell

ΔT = change in shell temperature

h = product height

In the measured product level, compensation was made as follows for the effects of both shell and product expansion and contraction:

$$T_{cv} = V - TV + TV_{sh}$$

where

T_{cv} = thermally compensated volume change

V = raw volume change measured by float-based level sensor

TV = change in volume due to thermal change in product

TV_{sh} = apparent change in volume due to thermal change in tank shell

THE MASS MEASUREMENT EXPERIMENTS

Mass measurement tests were performed with a bubbler-type differential-pressure-measurement system in which a gas is passed at a constant flow rate through a tube immersed in the product. The gas pressure in the tube must be high enough to overcome the hydrostatic head on the tube; the back pressure in the tube is therefore a measure of the hydrostatic head pressure on the bottom of the tube. In this experiment, two tubes having an inner diameter of 0.25 in. were used, one being the bubbler or "measurement" tube and the other a reference tube. The relative pressure in these two tubes was measured by a differential pressure gauge. (Because these gauges are typically very sensitive to temperature, a commercial refrigerator was used to maintain the gauge at approximately 4° C.) The pressure gauge, the refrigerator, and the nitrogen bottle that supplied gas to the measurement tube were all housed in a van parked about 150 ft from the AST. The measurement tube and the reference tube spanned this distance to enter the AST through a gauge port on its roof. From there, the reference tube opened into the region above the product surface. The measurement tube, however, was connected to a steel tube having the same inner diameter; this steel tube extended downward into the product, to a point approximately 10 in. from the tank floor. (The location of the gage ports in each of the three tanks is shown in Figure 1.) The temperature of the tank shell was monitored by a thermistor array consisting of four elements spaced at 90-degree intervals around the circumference of the tank. This information was used in the data analysis to compensate for thermal expansion/contraction of the tank shell.

THE MASS BALANCING EXPERIMENTS

The last type of volumetric test, conducted on Tank 9, was based on mass balancing techniques. In mass balancing, a differential pressure sensor measures the difference in head pressure between the product held in the tank and a column of product of equal height contained in a vertically oriented tube located outside the tank. In this experiment, two taps were drilled directly into the tank shell, approximately 6 in. and 60 in., respectively, above the tank floor. The lower tap opened into the product, while the upper tap opened at a level 5 in. above the product surface. The vertical tube containing product was connected to the upper and lower taps by two horizontal sections of piping. This setup is illustrated in Figure 2. A third tap installed at the same level as the lower tap was used to drain product and as the installation point for a second differential pressure measurement system.

No compensation for thermal effects was applied to the data from these tests.

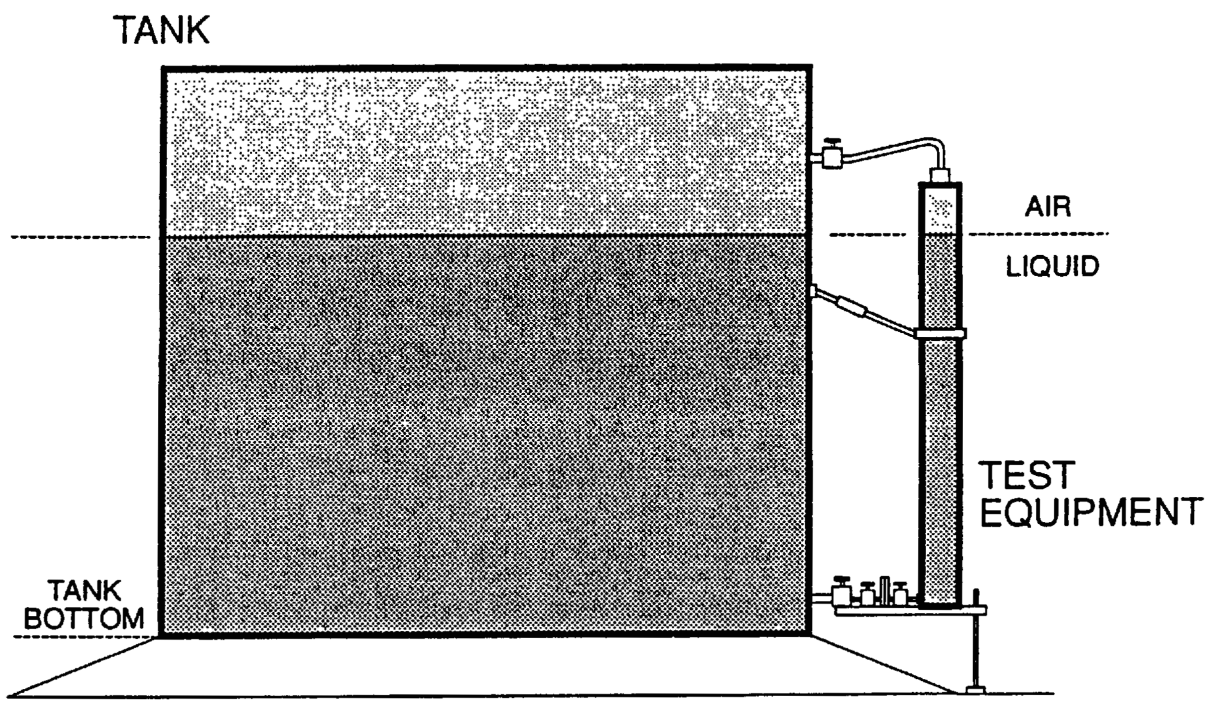

Figure 2. Configuration of the equipment used in the mass balancing tests.

RESULTS

Based on the results of tests conducted, none of the three tanks is believed to be leaking. Specific results for each tank are discussed below.

CONTROL TANK

Tank 23, the control tank, was tested over a three-day period, from 16 to 18 March. As was mentioned earlier, a complete inspection of the tank bottom had just been carried out. On March 12, Tank 23 was filled with product to a level of 33.25 in. (the total volume in the tank was approximately 48,000 gal), and on March 15 valve blinds were installed. At this point 24 h was allowed for the settling of the tank wall and floors before the start of the testing. During testing, the floating roof of this tank was resting on its legs, approximately 4 ft above the product surface. Three volumetric tests were done on the control tank: a 72-h level-and-temperature test at low product level; a 72-h mass measurement test at low product level; and a mass measurement test at high product level.

In the level-and-temperature tests conducted at low product level, gross changes in the volume of product measured by the level sensor were approximately 110 gal, peak to peak, over the three-day period. Diurnal fluctuations in volume coinciding with fluctuations in ambient temperature were on the order of 40 to 50 gal over a 24-h period.

The raw level data shown in Figure 3 indicate a strong diurnal fluctuation and a downward trend over the last two days[1]. The calculated thermal volume (Figure 4) shows the same diurnal fluctuation, although the trend is much less pronounced. In the control tank, as was the case with the other two tanks, the influence exerted by thermal expansion of the tank shell (shown for the control tank in Figure 5) was much less than that exerted by the thermal expansion of the product.

---

[1] Note that in Figure 3, as well as in subsequent plots where time is shown in hours, "10" corresponds to 10:00 am on the first day of testing, "20" to 8:00 pm the on first day, "30" to 6:00 am on the second day, etc.

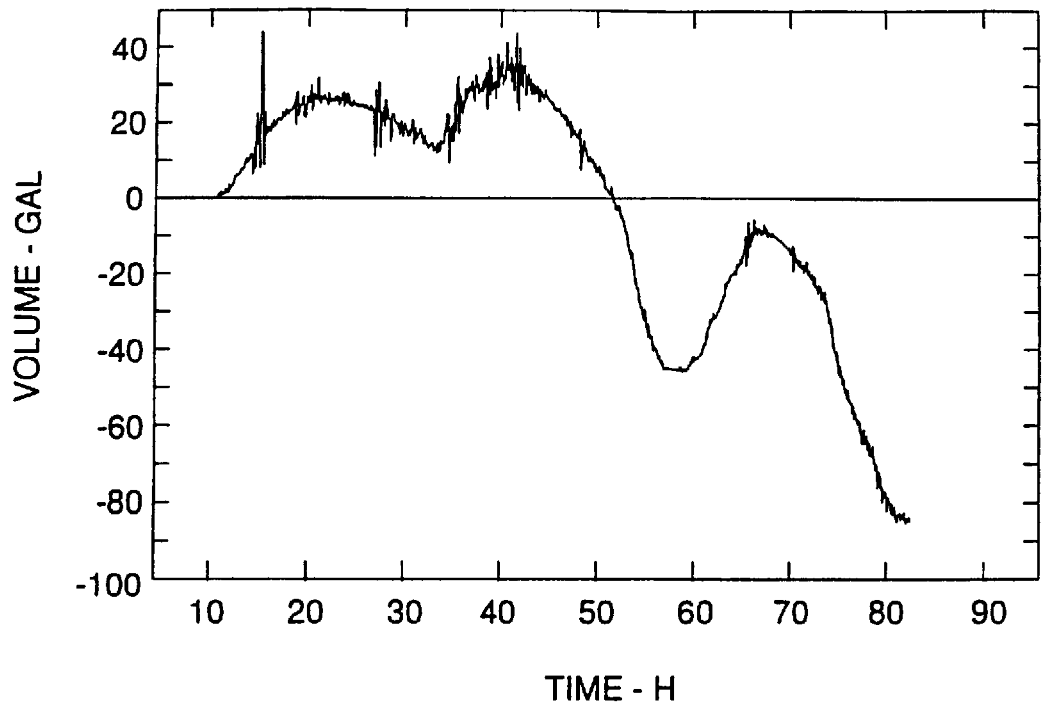

Figure 3. Measured product level (control tank).

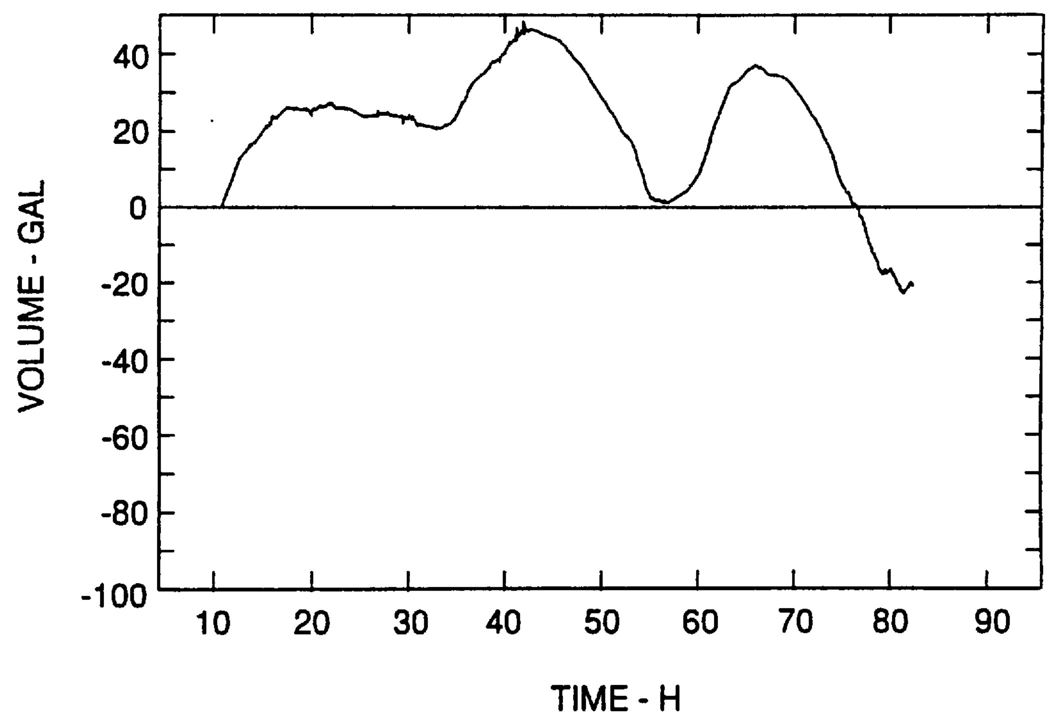

Figure 4. Thermal expansion of product (control tank).

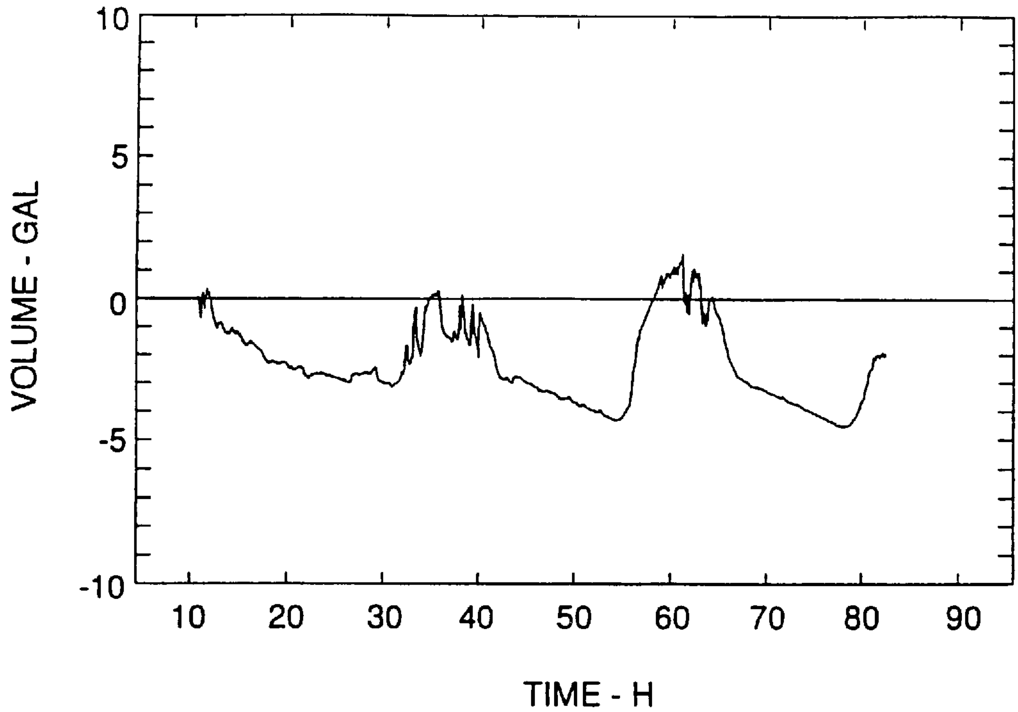

Figure 5. Apparent volume change due to shell expansion (control tank).

The temperature-compensated volume, shown in Figure 6, indicates an average outflow of approximately 1.1 gal/h over the three days.

A comparison of the calculated product expansion and the measured level changes shows that product expansion cycles match the measured level increases. Calculated product contraction, however, is much less than that indicated by the measured level data. Similar results were obtained during Phase III of this program, in tests conducted on a 114-ft-diameter AST instrumented with vertical arrays of thermistors near its wall and at its center. In those tests, thermal volumes were calculated from temperature measurements made at two locations: the center of the tank and the area near the walls. The two differed most significantly during periods when product temperature was decreasing. If heating and cooling of product are produced by different mechanisms, it is reasonable to suggest that horizontal gradients in the product are different in each case. The data from both Phase III and Phase IV indicate that the horizontal gradients in the rate of change of product temperature are less severe during periods of increasing

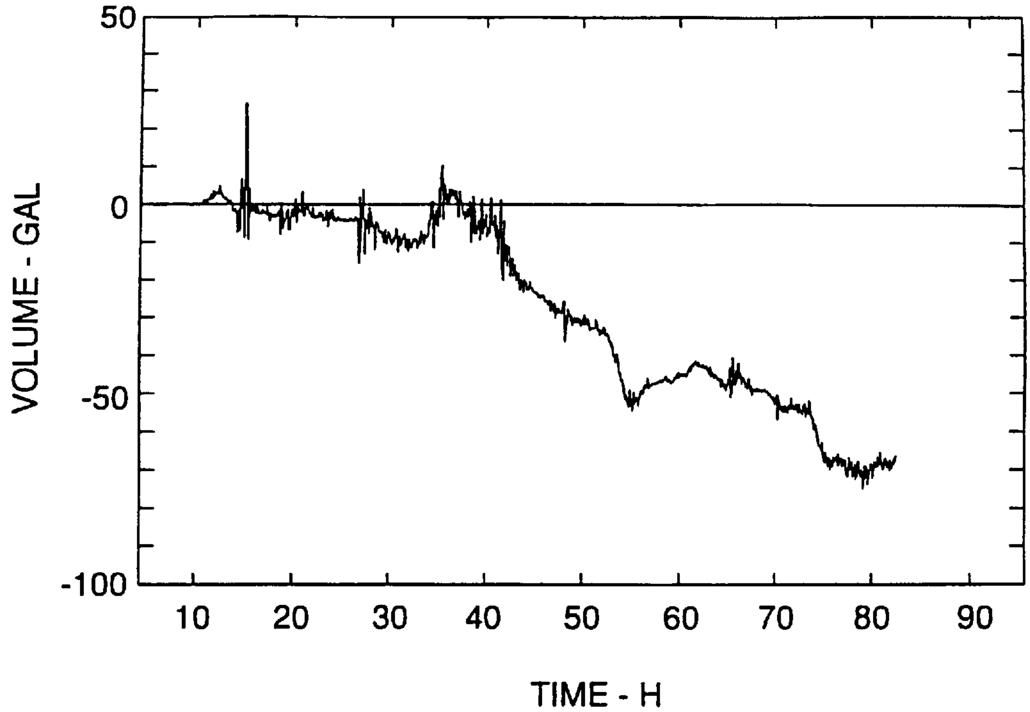

Figure 6. Compensated volume (control tank).

product temperature than they are during periods of decreasing product temperature (Vista Research, Inc., 1993).

The mass measurement tests conducted at low product level (over the same three-day period as the level-and-temperature tests described above) indicate an outflow of approximately 0.8 gal/h (Figure 7). The effect of thermal expansion in the 10 in. of product below the sensor was examined and was found to be minimal.

A possible explanation for the measured outflow is evaporative loss. Measured loss rates, however, are too high to be easily explained by evaporation and, furthermore, do not have the diurnal character that one would expect if evaporation were the cause. In subsequent tests, therefore, additional sensors were installed to monitor evaporation, ambient air temperature, and vapor space temperatures.

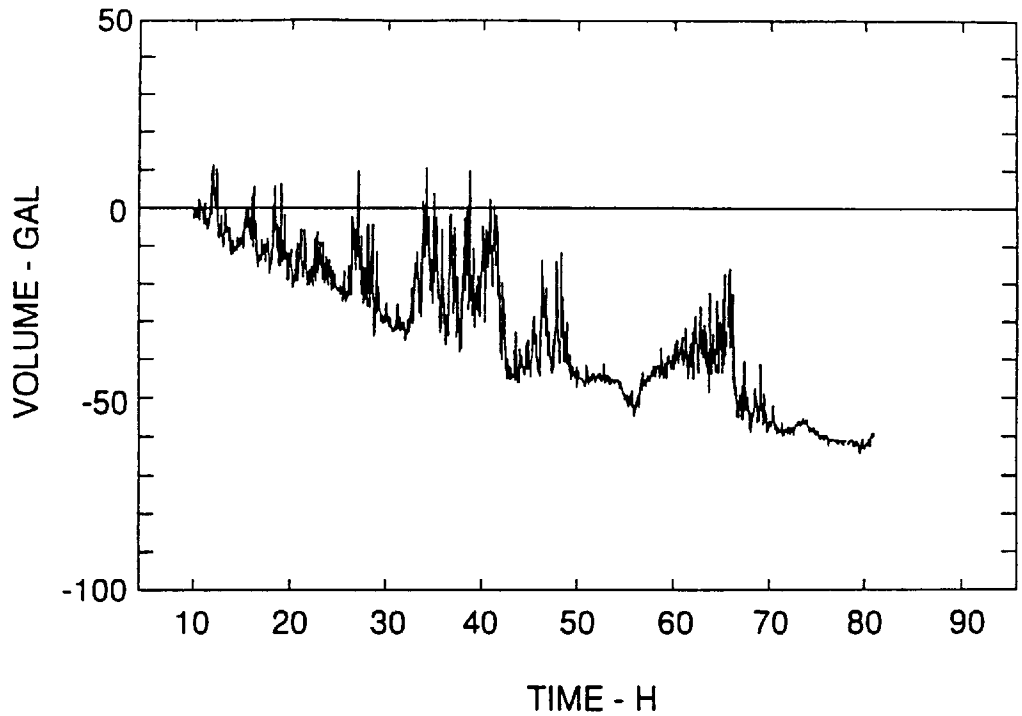

Figure 7. Mass measurements (control tank).

Mass measurement tests conducted at high product levels were inconclusive due to the effects of the floating roof resting on the product surface. These effects are discussed later in this paper in the section on the results of the Tank 2 tests.

TANK 9

Tank 9 underwent a 48-h volumetric test based on level and temperature measurements on 20 and 21 April. Product level had been lowered to 41.5 in. (the total volume in the tank was approximately 71,000 gal) and blinds had been installed on all valves 24 h before the start of testing.

In addition to the level sensor located inside the tank, this volumetric test employed a second level sensor whose purpose was to measure any evaporation that occurred during the test period. This second sensor was installed in an open-topped canister, 18 in. high and 4 in. in diameter, that was filled with product to a level of 14 in. The canister was configured so that the product it contained would be subject to the same thermal expansion and contraction, as well as the same rate of evaporation, as the uppermost 14 in. of product in the tank. The difference was that the canister would not be subject to any outflow of product resulting from a leak in the tank. Any outflow measured from the tank, therefore, could be compared to the measured rate of evaporation from the canister. A comparison of the two values would determine whether the measured outflow was the result of a leak, of evaporation, or a combination of both. The two-level-sensor configuration, shown in Figure 8, was used in the tests on Tank 2 as well as those on Tank 9.

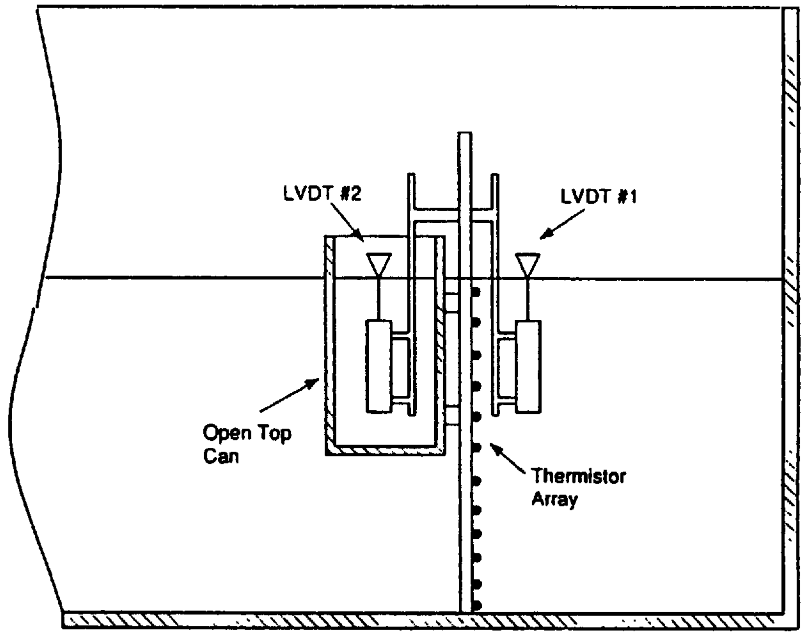

Figure 8. Two-level-sensor configuration for measuring evaporation.

The raw level data in Figure 9 clearly exhibit a diurnal cycle due to daily temperature fluctuations. Also evident are the points at which product was drained from the tank; this occurred ten times during the course of the test.

Figures 10 and 11 show the effects of the expansion and contraction of the product (these data include the ten "drains") and of the tank shell, respectively. Both figures were generated from data obtained by the thermistor array. Clearly, the product level, with daily fluctuations of 60 to

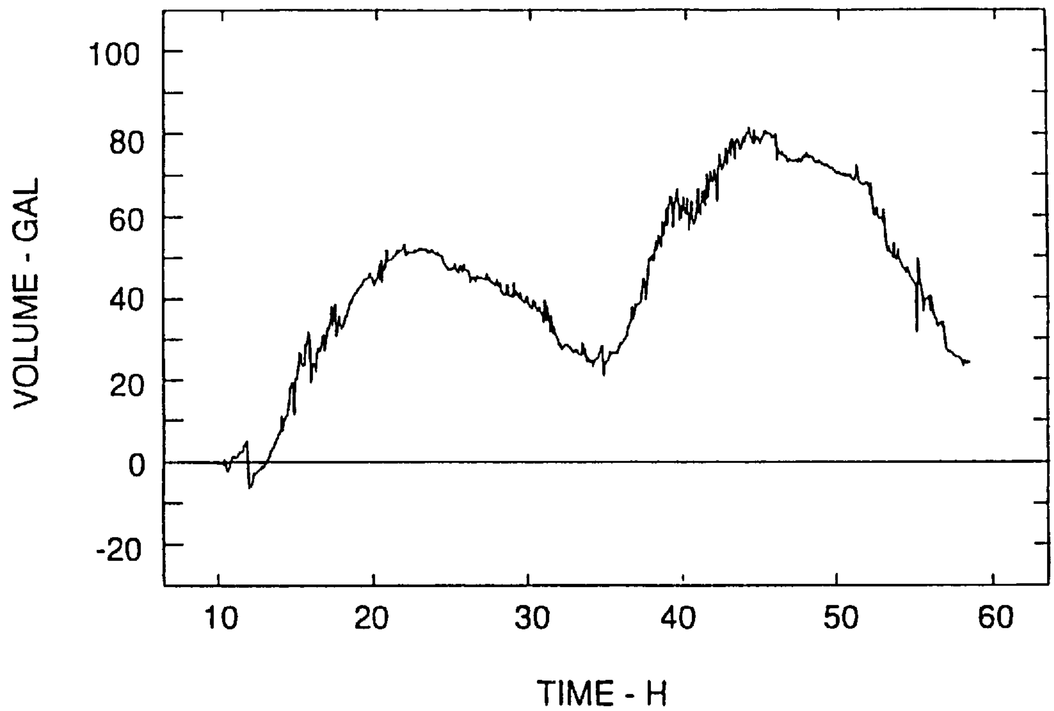

Figure 9. Measured product volume (Tank 9).

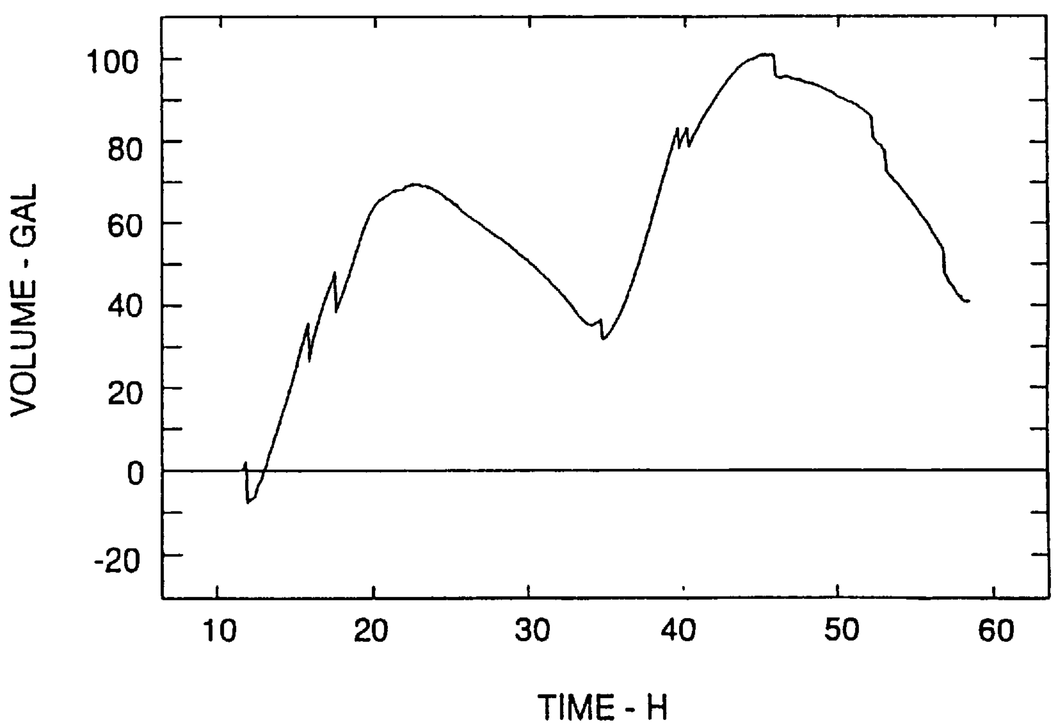

Figure 10. Effect of product expansion and product "drains" (Tank 9).

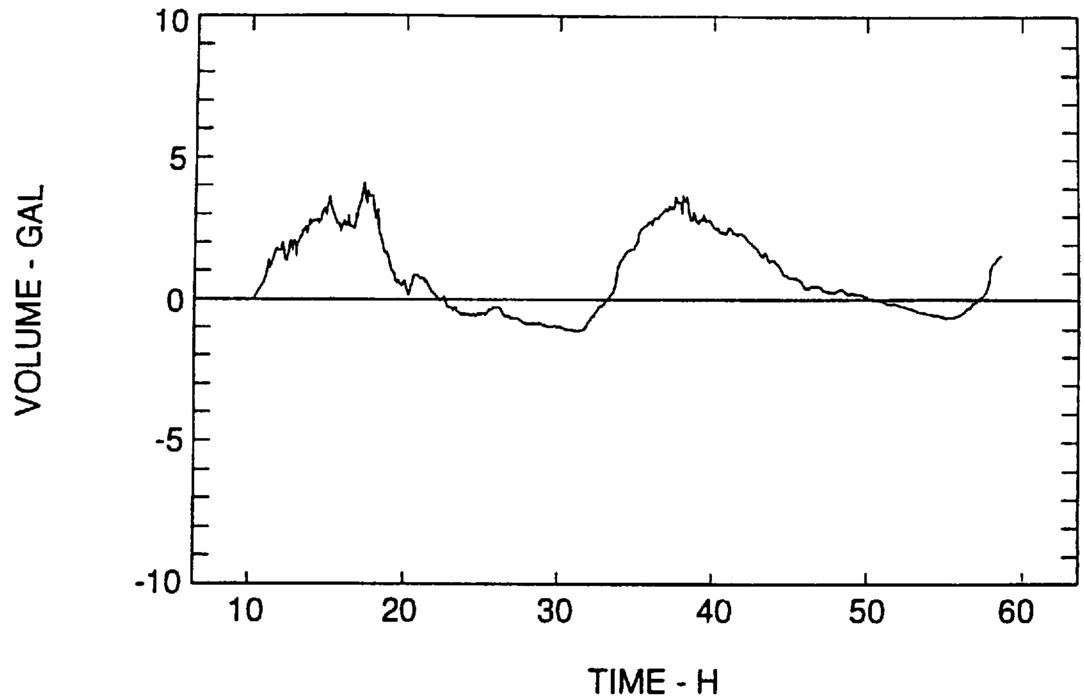

Figure 11. Apparent volume changes due to shell expansion (Tank 9).

70 gal, is dominated by the effects of product expansion. Product level is less affected by shell expansion, which causes apparent volume fluctuations of 5 gal or less (smaller by at least an order of magnitude than those caused by product expansion).

A comparison of the raw level data and the thermal volume data indicates a lag of about 1.75 h between the thermally induced volume changes and the level changes. This lag may be due to horizontal gradients in temperature within the tank. (Note that the vertical thermistor array was located near the wall of the tank.) If, as a result of ambient thermal influence, a significant portion of the heating and cooling of product occurs near the tank walls, one would expect that temperature changes would be greater in that region, and occur sooner there, than they would in the region near the center of the tank. Since the level of product is a function of the average temperature in the tank, changes in level will lag behind thermal changes measured near the tank wall.

A delay of 1.75 h was therefore imposed on the thermal volume data, which were then applied to the raw level data in order to obtain the temperature-compensated volume data. Since no lag time was anticipated between temperature changes in the tank shell and the associated level changes in the product, thermal volume data on the tank shell were applied, without alteration, to the raw level data. The resulting temperature-compensated volume data (Figure 12) show an average

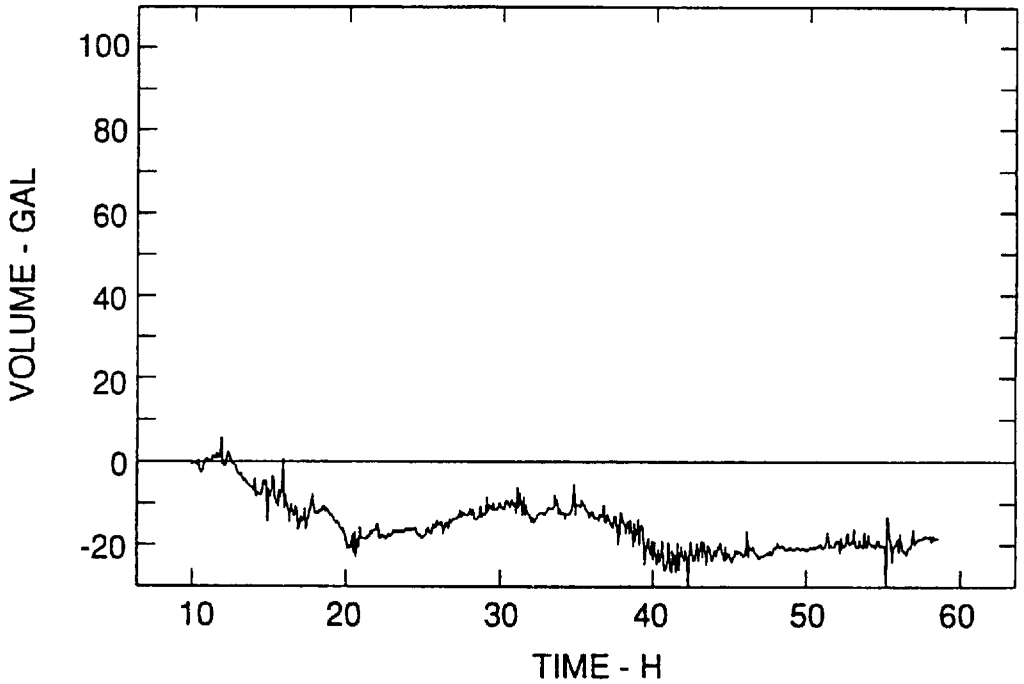

Figure 12. Compensated volume (Tank 9).

outflow of 0.38 gal/h. Also apparent in the data, however, is a residual diurnal effect whose characteristics appear directly opposed to those of the thermal volume. This is an indication of overcompensation for thermal expansion in calculating the level data. If indeed the temperature fluctuations near the center of the tank are less pronounced than those near the walls, the thermal volume calculated from measurements made by an array near the walls would be overstated. It appears that the actual volume changes were only 85% of those calculated from the measured temperature of the product. When a reduced thermal volume is applied to the level data (Figure 13), the results show a greatly reduced residual diurnal cycle and no significant flow into or out of the tank.

Both the time delay and the attenuation factor used in this analysis were based on data collected as part of the level-and-temperature-based volumetric test on Tank 9. These two values are important only in that they are evidence of horizontal gradients in the temperature of the product; such gradients, if not considered in the data analysis, will degrade the performance of any volumetric test based on level and temperature measurements.

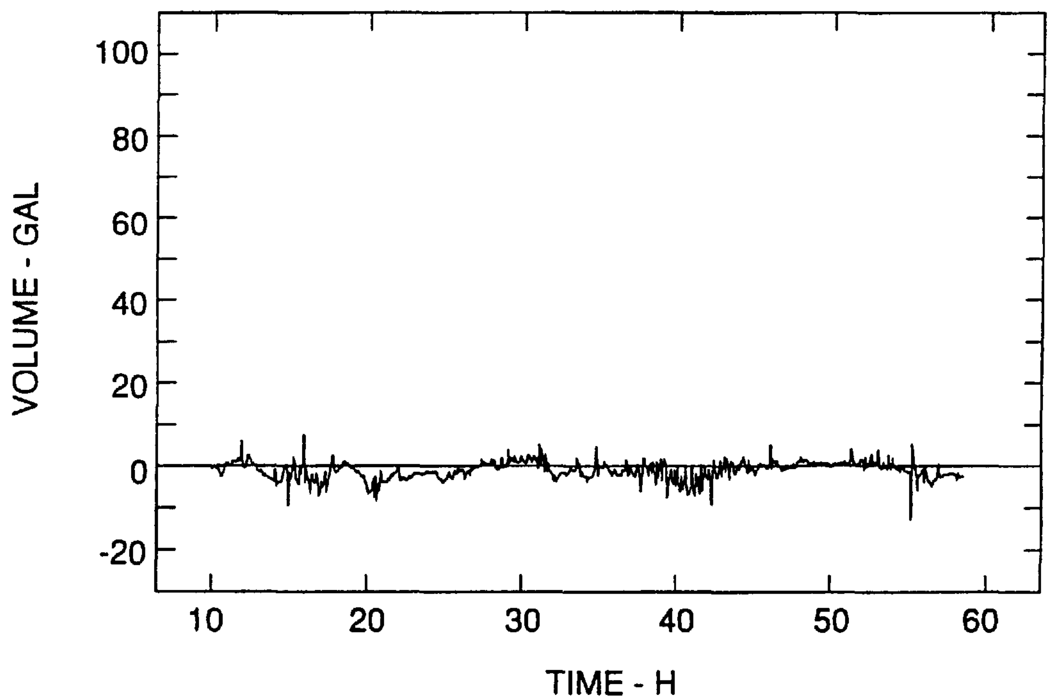

Figure 13. Volume compensated with reduced thermal effect (Tank 9).

The temperature-compensated volume measured by the second level sensor in the open-topped canister, as seen in Figure 14, showed no indication of a dominant evaporation effect during the test period.

On the first day no evaporation or condensation occurred during the period from 0945 (the start of the test) to 1430; on the second day none occurred between 0800 and 1230. During the rest of the test, condensation in the canister was steady at a rate of approximately 2 x 10^{-4} gal/h. Because condensation is not purely an artifact of the surface area (indeed, in the canister the bulk of the measured condensation is believed to have occurred along the inner walls rather than at the

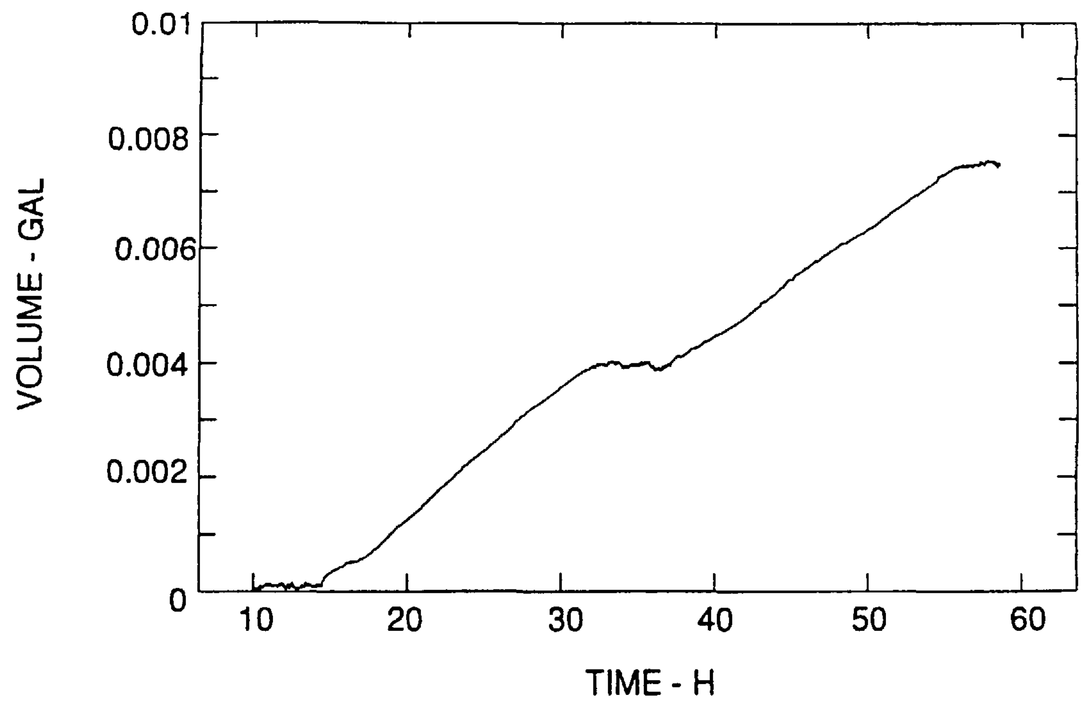

Figure 14. Compensated volume in canister.

interface between air and product), the measured increase in the volume of product in the canister cannot in this case be extrapolated in order to predict the amount of condensation occurring in the tank.

A volumetric test based on mass measurement techniques was conducted on Tank 9 during the same period as the volumetric test based on level and temperature measurements. These mass measurement data, compensated for thermal expansion of the tank shell, are shown in Figure 15. As in the level-and-temperature data, product "drains" are visible. When the effect of these "drains" is removed (Figure 16), the data indicate a relatively steady inflow into the tank of approximately 1.7 gal/h. Two possible causes for this inflow were investigated.

The first possibility was thermal expansion of the product in the region below the measurement tube. Based on an initial level-gauge reading of 41.5 in. of product and on a corresponding initial pressure reading from the mass measurement system of approximately 27 in. H_2O (32.1 in. of turbine fuel), it was assumed that the lower end of the measurement tube was 9.4 in. from the

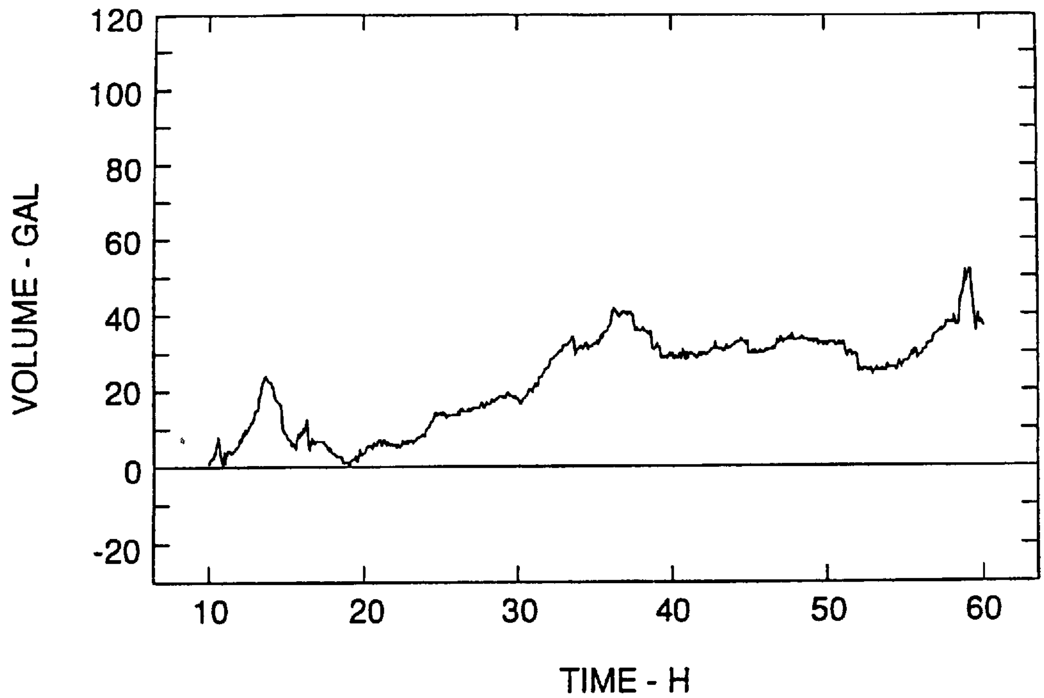

Figure 15. Mass measurement of volume (Tank 9).

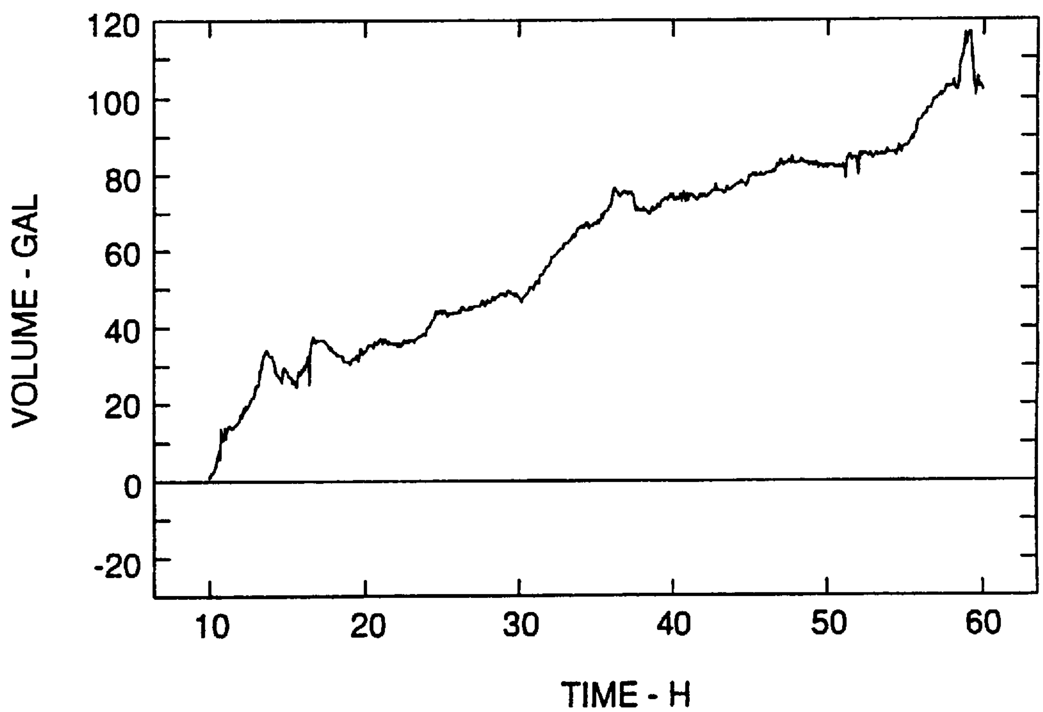

Figure 16. Mass measurement data compensated for product "drains" (Tank 9).

bottom of the tank. Temperature data taken as part of the level-and-temperature measurements were then used to calculate the amount of thermal expansion in the bottom 9.4 in. of product. As illustrated in Figure 17, the thermal volume in this region of the tank increases steadily over the course of the two-day period and accounts for approximately 0.36 gal/h of the inflow indicated in the uncompensated data.

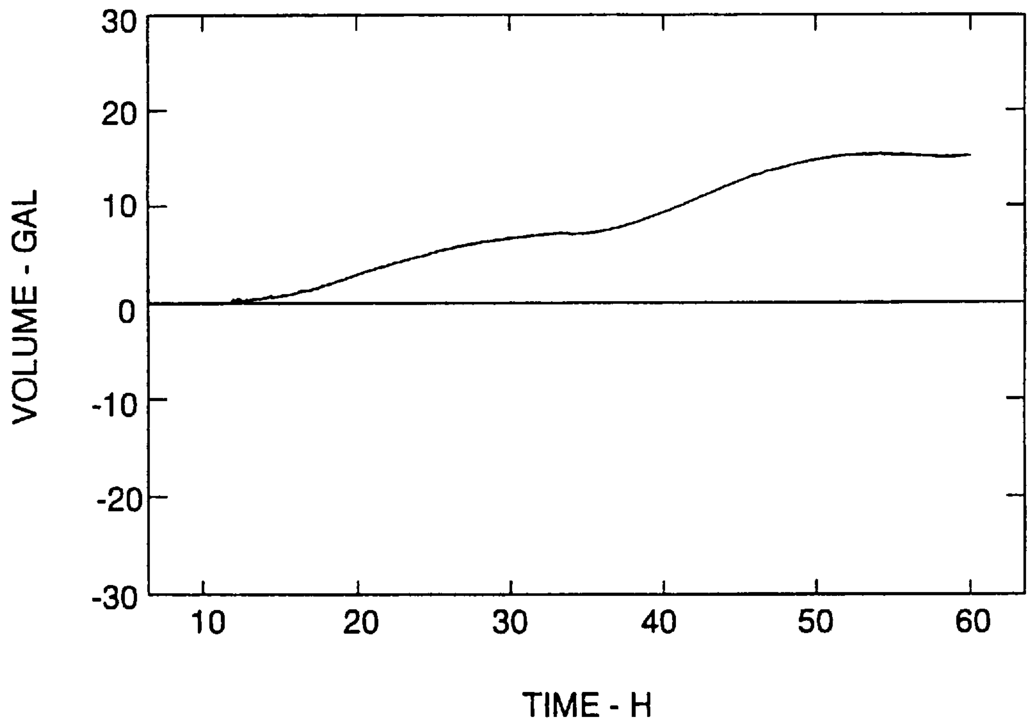

Figure 17. Thermal volume change in the bottom 9.4 in. of product (Tank 9).

The second possibility was that of thermally induced fluctuations in the viscosity of the gas used in the bubbler tubes. The drop in pressure between the two ends of the bubbler tube (the end to which the nitrogen bottle was attached and the end that opened into the product) can be described by the following equation:

$$p = \frac{8l\eta v}{\pi r^4}$$

where

p = pressure drop from one end of the tube to the other

l = length of the tube

η = coefficient of viscosity of the gas in the tube

v = flow rate of the gas in the tube

r = inner radius of the tube

Because viscosity is a function of temperature, the pressure drop across a tube containing gas under flow will also vary with temperature. Within the range of temperatures encountered during these tests, the viscosity of nitrogen varies linearly with temperature at a rate of 0.047 lb/(h·ft·deg C). For the purpose of calculating the thermal effect on viscosity, it was assumed here that the rate of flow in the measurement tube was 0.2 ft^3/h. Given this flow rate, the length of the tubes (150 ft of tubing outside the tank and 38 ft inside), and the inner diameter of the tubes (0.25 in.), the measurement error for Tank 9 is approximately 0.8 gal/deg C. Temperature in the tubes was estimated from measurements made by three thermistors, one located outside the tank, in a shaded area, and two located inside the tank in the vapor space above the product. The estimated thermal effect on viscosity over the duration of the test period is shown in Figure 18. Although there is no long-term trend in these data that might explain the measured inflow, the effects of changes in N_2 viscosity are apparent. While they are greatest during daylight hours, fluctuations in pressure are also observed at night, during which periods they can produce errors of nearly 2 gal/h.

When both of the above possibilities are compensated for, the data still show an inflow into the tank of approximately 1.5 gal/h throughout almost the entire test period (Figure 19). A number of other factors not investigated here may be responsible, among them temperature drift in the differential pressure sensor, or condensation (which implies errors in the level and temperature measurements). There are insufficient data to either confirm or rule out these possibilities.

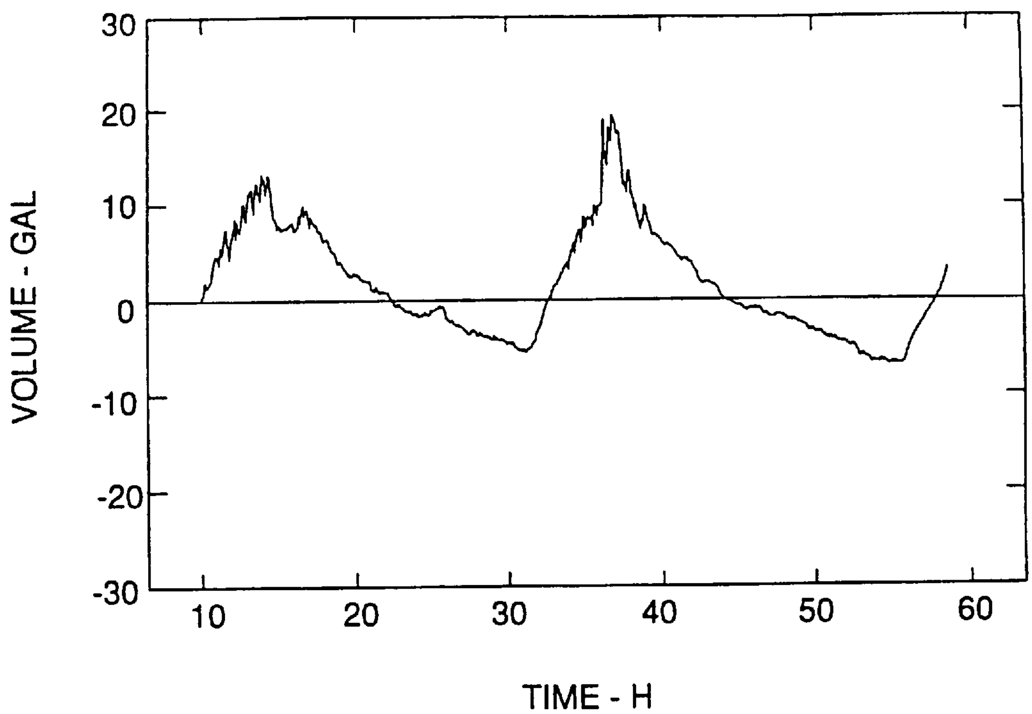

Figure 18. Apparent volume change due to thermally induced changes in the viscosity of nitrogen gas used in the bubbler tubes (Tank 9).

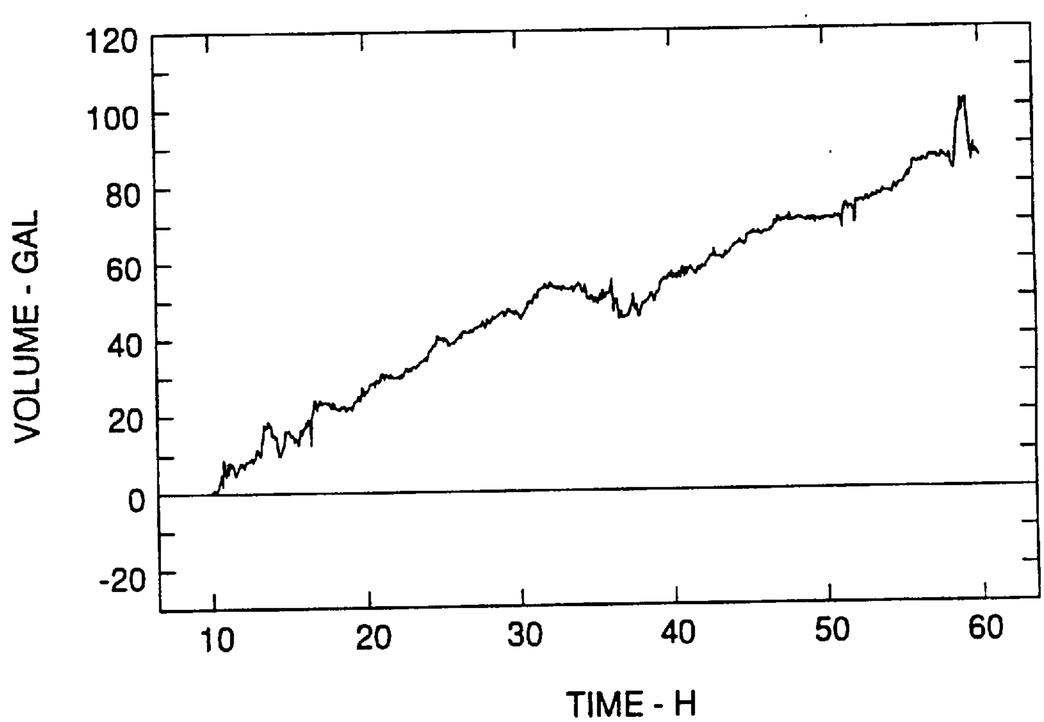

Figure 19. Compensated data from mass measurement tests.

In addition to the level-and-temperature and the mass-measurement tests conducted on Tank 9, a number of 4-h mass balancing tests were done throughout the two-day period. A large number of these data sets were contaminated because of the fact that direct sunlight heated the differential pressure sensor. The only data that were analyzed, therefore, were those collected between 0400 and 0830 (a period when sunlight was not a factor) on 22 April. During this period there were two mass balancing systems on Tank 9, and data were collected concurrently by both. Flow rates measured by the two systems were -0.96 gal/h and +2.7 gal/h, respectively. Tank shell temperatures measured during the two-day test period varied enough to suggest that expansion of the shell alone will cause apparent volume changes that, over a period of 4 h, would appear as constant flow rates. Depending on the time of day, the measured flow rate as influenced by shell expansion would be between +1 and -1 gal/h. More pronounced than the influence of shell expansion, however, was that of the heating of the differential pressure sensor and the stand pipe. It is reasonable to believe that data collected at night are also strongly affected by thermal changes in the test equipment (Vista Research, Inc., 1993). Because the mass balancing data sets were only 4 h in duration, it is not possible to determine from this data set the magnitude of the thermal influence on the test equipment; to do this one would need a continuous data set collected over a period of at least 24 h.

TANK 2

A level-and-temperature-based volumetric test was conducted on Tank 2 over a 48-h period beginning on 1 May. The roof of this AST was floating on the product surface during testing. Product level was 54.75 in. at the manway where the thermistor array was installed (total volume in the tank was approximately 130,000 gal).

The measured product level, shown in Figure 20, varies by more than 0.25 in. over the course of the test. Under the assumption that the floating roof moves up or down freely with the surface of the product, the level data were compensated for thermal expansion of the product and of the tank shell. The resulting temperature-compensated volume is shown in Figure 21. Large, rapid

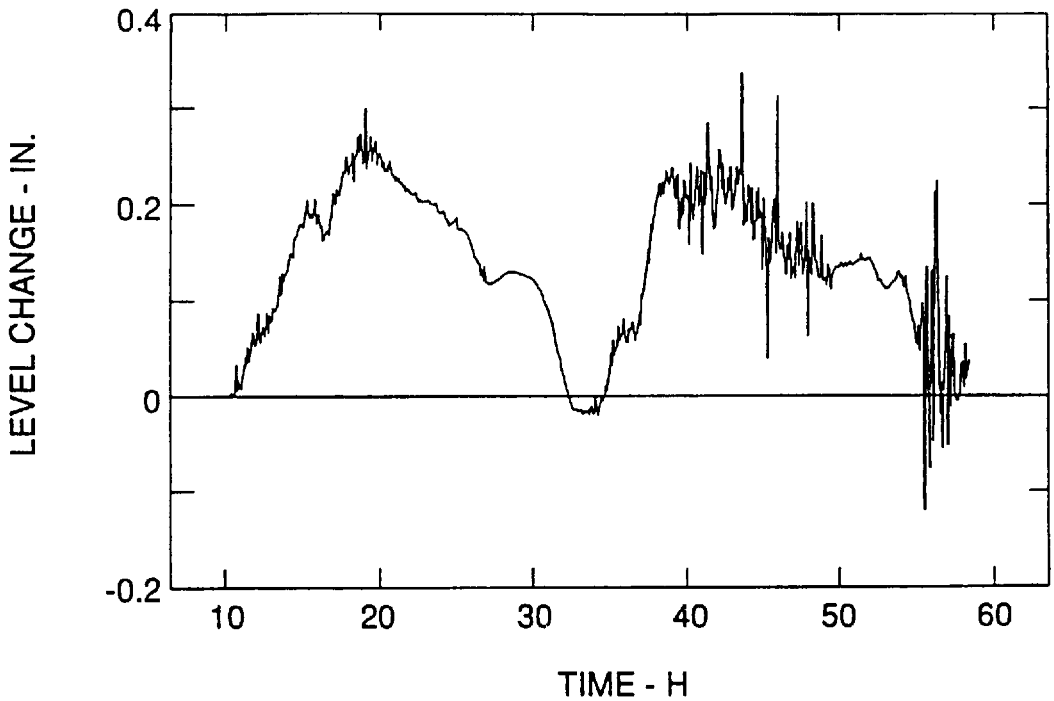

Figure 20. Measured change in product level (Tank 2).

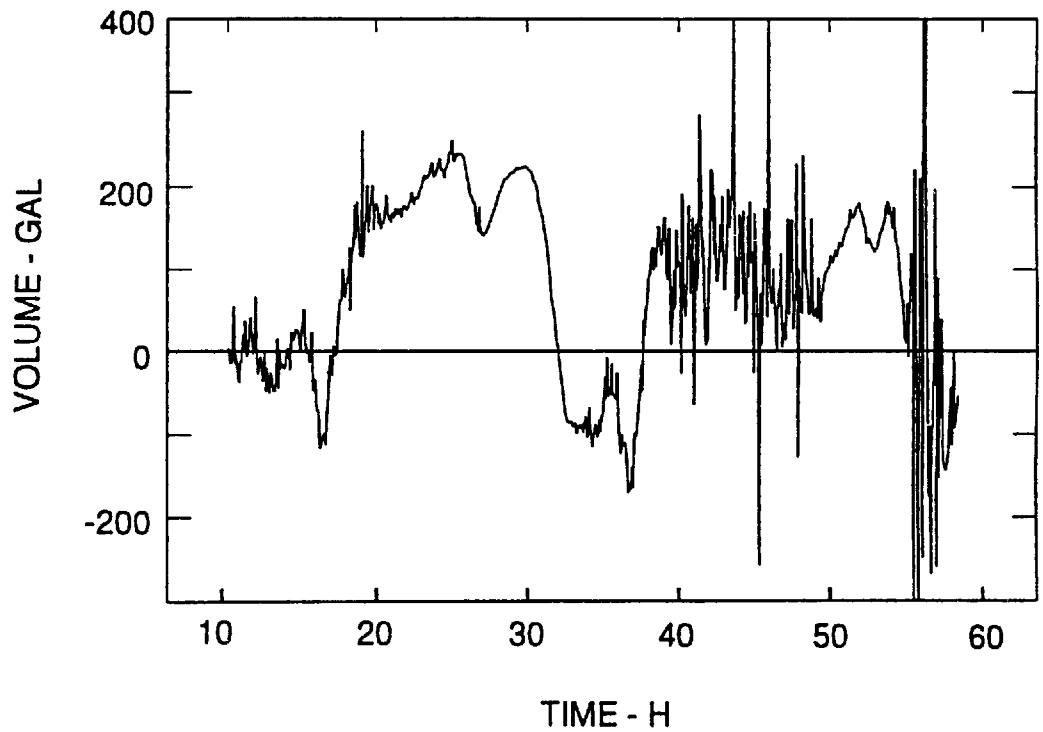

Figure 21. Temperature-compensated volume (Tank 2).

volume changes (200 to 300 gal over a 2- to 3-h period) occur twice each day during the two-day test, and the times at which they occur coincide with the minimum and maximum thermal volumes (shown in Figure 22) for each day. These discontinuities may be explained by changes in the characteristics of roof motion. As the rate of expansion of the product decreases, the force exerted by the product against the roof also decreases. Eventually, this force becomes insufficient to overcome frictional forces between the roof and the tank walls. At this point the roof stops moving, but the product continues to expand into the manways and the annular space between the perimeter of the roof and the wall of the tank. During periods when roof motion stops, assumptions about the relationship between changes in product height and changes in product volume become invalid. It is during these periods that the very large, *apparent* volume changes described above appear in the data.

Mass measurements made at a high product level in Tank 2 and the control tank (Figures 23 and 24, respectively) were also subject to the characteristics of roof motion. Because this effect was dominant, it was not possible, based on these data, to evaluate the effect of a high product level on test performance.

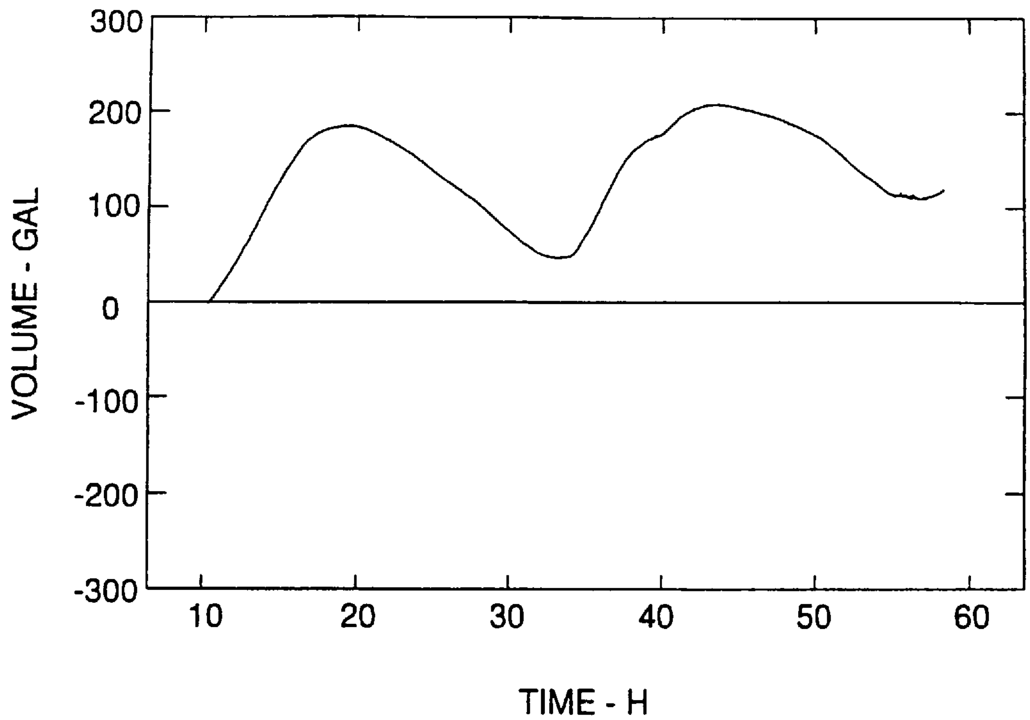

Figure 22. Thermal expansion of the product (Tank 2).

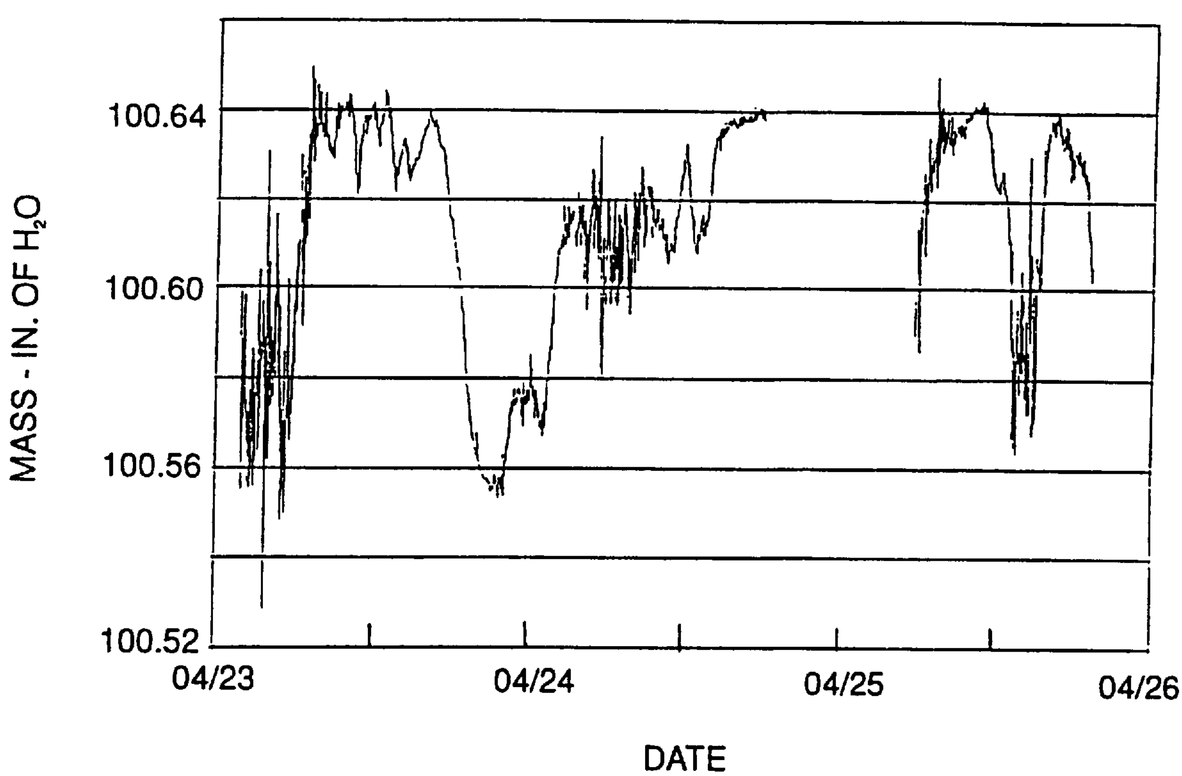

Figure 23. Data from mass measurement test at high product level (Tank 2).

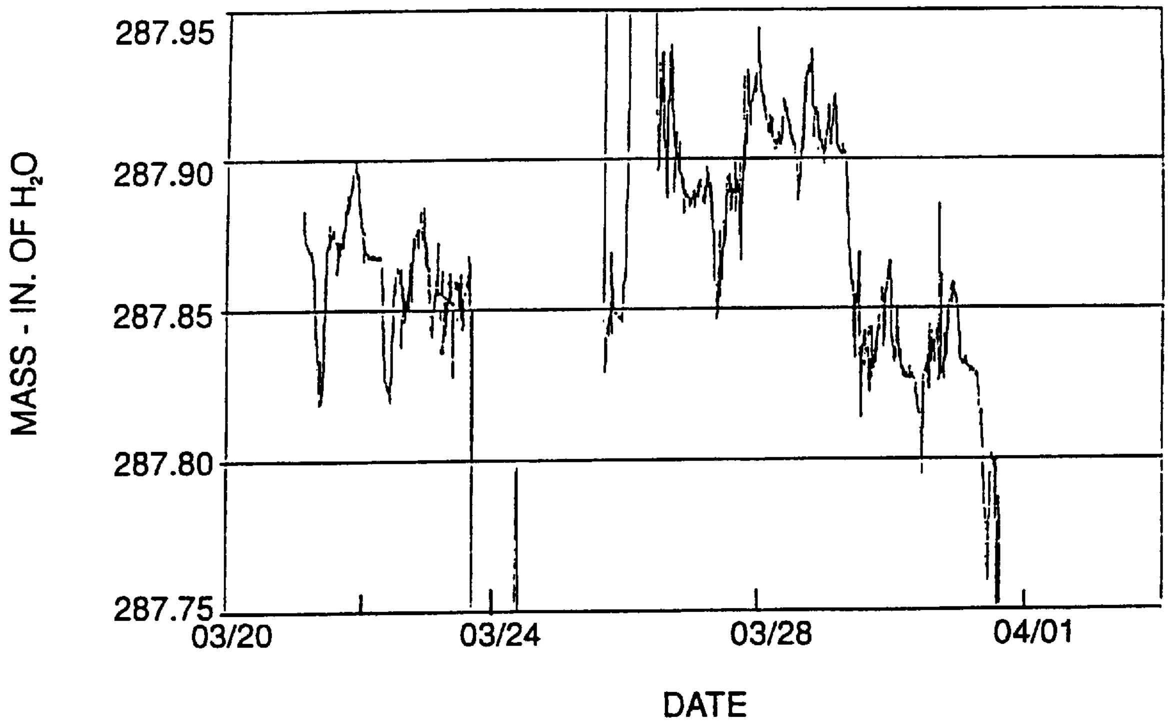

Figure 24. Data from mass measurement test at high product level (control tank).

DISCUSSION

Three sources of noise that affect the accuracy of volumetric tests were investigated during the above-described series of tests: a roof floating on the product surface, evaporation and condensation, and temperature fluctuations.

The success of a volumetric test depends on accurate knowledge about the relationship between changes in the level and changes in the volume of product. When a roof is floating on the product surface, external forces such as friction, wind and rain can alter this relationship and thereby cause errors in volumetric measurements. It was seen during this series of tests that these forces were sufficiently large to preclude accurate testing of a floating-roof AST *while its roof is resting on the product surface.*

An attempt was made during this test series to quantify evaporation in two of the ASTs tested. No significant evaporation was measured in either case. It was found, however, that condensation within the canister used to measure evaporation may have precluded an accurate assessment of evaporation within the tank. Further work is required for a better understanding of the effects of evaporation and condensation on the accuracy of volumetric tests. Once the magnitude of these effects is known, the need to measure and compensate for evaporation and condensation can be evaluated, and volumetric tests that quantify these phenomena as part of their protocol can be developed.

As had been determined in Phases II and III of the program, it was found in Phase IV that all volumetric tests were affected by temperature changes occurring during the test period (Vista Research, Inc., 1993). There are two ways of mitigating the effects of temperature on test performance. One is by compensating for temperature directly on the basis of measured temperature changes and their calculated effects. The other is by differentiating the thermal effects from the leak signal.

Temperature compensation requires that there be a well known relationship between temperature and its effect on measured volume; sufficient temperature information must be recorded during the test to accurately estimate its effect. Thermal effects can be differentiated from the leak signal by exploiting the fact that volumetric changes due to a leak will be time-invariant, while changes due to thermal effects will vary over time. In order to make this differentiation, the duration of the test must be longer than the period of thermal variation. Although neither method will eliminate the influence of temperature changes on test results, significant improvements in test performance can be achieved when one or both of these methods can be applied.

Three mechanisms have been identified which can cause the thermal effects seen in the volumetric tests in this series: (1) product expansion and contraction; (2) AST shell expansion and contraction; and (3) measurement error due to thermal effects on instrumentation. The three types of volumetric test examined in this series are affected to some degree by all three of these mechanisms.

To design a test capable of differentiating these mechanisms from the leak signal, one must know the period of fluctuation for each mechanism. The period of fluctuation is driven by the period of ambient temperature change, which has two predominant modes: the diurnal cycle, which typically exhibits the greatest range in the rate of temperature change; and the changes associated with weather conditions, which occur over a period of days or weeks. Clearly, the test durations required to differentiate the latter changes from the leak signal are operationally impractical; however, the rate of change of temperature over a period of days or weeks is typically low in comparison to diurnal changes, so that, in a well-designed test, temperature compensation is sufficient to reduce the effects of long-term temperature changes to acceptable levels. The duration of the test must be greater than one diurnal cycle because the larger diurnal fluctuations are not sufficiently attenuated by temperature compensation. The long test period is required so that residual diurnal effects can be differentiated from the leak signal.

CONCLUSIONS AND RECOMMENDATIONS

The importance of effective thermal compensation and long test durations was evident from the data collected during this test series. The effectiveness with which each type of volumetric test handled the noise mechanisms is described below, and recommendations are given for further studies that might improve the performance of each type of volumetric test.

LEVEL-AND-TEMPERATURE TESTS

The performance achieved by level-and-temperature tests in this series is consistent with that achieved in Phase III: in 48-h tests, a leak rate of 1 gal/h is detectable (Vista Research, Inc., 1993). As in Phase III, the greatest source of noise was thermal expansion of the product. The relationship between measured volume changes and fluctuations in product temperature is well established and can be accurately modeled if sufficient data on product temperature are available. It was seen during this test series that a single vertical thermistor array does not provide enough information to completely characterize the temperature of the product, since the rate of temperature change varies horizontally within the product. In tanks that have large diameters, such as ASTs, lack of adequate temperature characterization can have a profound effect on test reliability. Horizontal gradients in one of the two ASTs tested were great enough to cause errors of 15% in temperature compensation. In order for a test to reliably detect leaks as small as 1 to 2 gal/h, it is necessary to have a number of vertical arrays that are horizontally separated. The number of arrays, and the required spacing between them, can not be determined from the data collected during this test series. Studies should be conducted on the variability in thermal rates of change as a function of horizontal position in an AST. In this way, it will be possible to assess the operational feasibility of thermal measurements, and the potential performance gain derived from them.

The effects of thermal expansion and contraction of the AST shell were apparent in the data collected in each of the two level-and-temperature tests. Although the relationship between shell temperature and the apparent change in tank volume is only approximated, the effect of shell expansion is at least an order of magnitude smaller than that of product expansion. The effect is dominantly diurnal, and, when test durations are greater than 24 h, contributes errors in volume rate calculations of much less than 1 gal/h. Therefore, even temperature compensation that is only 70 to 80 percent effective, when combined with test durations longer than one diurnal cycle, sufficiently reduces the effect of this error, to the point that it is not a limiting factor in test accuracy. Compensation for thermal expansion and contraction of the tank shell, as applied in this test series, is believed to have been adequate.

MASS MEASUREMENT TESTS

The low-product-level mass measurement tests were affected by noise sources different from those that affected the level-and-temperature tests. The performance of these two types of volumetric tests was nevertheless roughly equivalent. Mass measurement tests are not affected by thermal expansion and contraction of the product in the region above the measurement point. In one of the two tanks tested, however, product expansion below the measurement point (which was 10 in. above the tank floor) was a significant source of error. In this case, the effect of the error was reduced through temperature compensation based on data from the level-and-temperature tests. Placing the measurement point closer to the tank floor would also have reduced the impact of the error; this may not always be possible, however, because if there is a layer or water or sludge at the bottom the tank, placing the measurement point within this layer would severely degrade measurement accuracy. The primary source of noise appeared to be thermal influences on the instrumentation. The effect of thermally induced changes in the viscosity of the nitrogen gas used in this tube was detectable in the data. Again, thermal compensation based on the level-and-temperature measurements was applied. A better way to mitigate this effect, however, is to equalize the air flow in the reference and measurement tubes. When the air flow is equalized, both tubes are subject to identical pressure fluctuations due to changes in the viscosity of the gas, and therefore measurements of the pressure differential between the two tubes will not be affected. That fact that differential pressure sensors are temperature-dependent is known to be a significant source of error in mass measurement tests. Based on previous tests conducted with a number of differential pressure sensors, the error is thought to be as high as 0.01 in./°C (20 to 30 gal/°C). Given the high susceptibility of this equipment to thermal conditions, either one or both of the following should be done: the temperature of any differential pressure sensor used during a test should be tightly controlled, or the temperature of the sensor should be monitored so that thermal changes can be compensated for. In this series of tests, the temperature of the differential pressure sensor was controlled by means of a commercial refrigerator. The data from this test are insufficient to quantify the error due to the thermal response of the differential pressure sensor. It is believed, however, that test performance can be improved by the incorporation of tighter temperature controls and/or temperature compensation.

As in the level-and-temperature tests, thermal compensation for the expansion and contraction of the AST shell was adequate. It reduced the impact of this mechanism sufficiently that shell expansion/contraction was not believed to be a limiting factor in test performance.

MASS BALANCING METHOD

The mass balancing test, as implemented on Tank 9, was subject to most of the same sources of noise as the mass measurement test. There were two significant differences in methodology, however, that severely degraded the accuracy of the mass balancing test. First, there was no attempt in the mass balancing test to control or compensate for the temperature response of the differential pressure sensor or to compensate for expansion of the AST shell. Shell expansion alone can affect the measurement of the rate of change of product level by 1 to 2 gal/h over short periods. The effect of the heating and cooling of the differential pressure sensor may be even greater, exceeding that of shell expansion by an order of magnitude. The second difference is that the duration of the mass balancing test was only 4 h. Because the test duration was so much shorter than a diurnal cycle, it was impossible to differentiate between thermal mechanisms and a leak. The performance of a mass balancing system can be at least as good as that of a level-and-temperature or a mass measurement system. The test procedure used during this series, however, failed to address significant sources of noise. The short test period and the lack of temperature compensation made the results difficult to interpret and allowed the detection of large leaks only.

REFERENCES

Vista Research, Inc. 1991. *An Engineering Assessment of Volumetric Methods of Leak Detection for Aboveground Storage Tanks*. API Report No. 306. American Petroleum Institute. Washington, D.C.

Vista Research, Inc. 1993. *An Engineering Evaluation of Volumetric Methods of Leak Detection for Aboveground Storage Tanks*. API Report No. 323. American Petroleum Institute. Washington, D.C.

Order No. 849-32500

104PP

05944C1P

RELATED API PUBLICATIONS...

PUBL. 322 — *An Engineering Evaluation of Acoustic Methods of Leak Detection in Aboveground Storage Tanks*
January 1994

PUBL. 322 — *An Engineering Evaluation of Volumetric Methods of Leak Detection in Aboveground Storage Tanks*
January 1994

To order, call API Publications Department (202) 682-8375

American Petroleum Institute
1220 L Street, Northwest
Washington, D.C. 20005